UNIVERSITY OF KASDI MERBAH OUERGLA

Faculty of Hydrocarbons, Renewable Energies, Earth and Universe Sciences

Department of Drilling and Oilfield Mechanics

Thesis Master Professional

Field: science and technology

Sector: hydrocarbons

Specialty: Drilling

Presented by: Zouari Ahmed Souhaib, ***Si Hamdi Mohamed El-Amine*** and ***Slimani Ziad***.

Theme:

Investigating the influence of fluid rheology and multiphase flow on pressure and flow dynamics in non-Newtonian wellbore systems

Publicly supported on **dd/MM/2024**

In front of the jury:

Mr. Toumi Nabil	President	U.K.M Ouargla
Mr. Abidi Saad Elfakeur	Supervisor	U.K.M Ouargla
Mr. Hachana Oussama	Examiner	U.K.M Ouargla

Academic year 2023/2024

Abstract:

This thesis investigates the influence of fluid rheology and multiphase flow on pressure and flow dynamics in non-Newtonian wellbore systems, with a specific focus on the parameters affecting pressure losses. One of the major parameters examined in this study is eccentricity, which refers to the offset between the wellbore and the drill string. Non-Newtonian fluids, characterized by their complex viscosity behavior, present unique challenges in wellbore operations, particularly in drilling, production, and completion processes. Key parameters such as fluid viscosity, shear rate, flow velocity, pipe geometry, and especially eccentricity are systematically analyzed. The findings reveal that eccentricity significantly affects pressure losses by altering flow patterns and increasing frictional forces within the annulus. Eccentricity leads to asymmetric flow distribution, which in turn impacts the overall pressure gradient and efficiency of fluid transport. Results highlight the necessity for accounting for eccentricity in the design and operation of wellbore systems. The study provides practical insights into optimizing drilling and extraction processes, aiming to minimize pressure losses and improve operational efficiency. By enhancing the understanding of how eccentricity and other parameters influence pressure dynamics, this research contributes to safer and more cost-effective wellbore operations.

Résumé :

Cette thèse étudie l'influence de la rhéologie des fluides et de l'écoulement polyphasique sur la pression et la dynamique de l'écoulement dans les systèmes de puits non newtoniens, avec un accent particulier sur les paramètres affectant les pertes de charge. L'un des principaux paramètres examinés dans cette étude est l'excentricité, qui fait référence au décalage entre le puits de forage et le train de tiges. Les fluides non newtoniens, caractérisés par leur comportement complexe en viscosité, présentent des défis uniques dans les opérations de forage de puits, en particulier dans les processus de forage, de production et de complétion. Des paramètres clés tels que la viscosité du fluide, le taux de cisaillement, la vitesse d'écoulement, la géométrie du tuyau et surtout l'excentricité sont systématiquement analysés. Les résultats révèlent que l'excentricité affecte de manière significative les pertes de charge en modifiant les schémas d'écoulement et en augmentant les forces de frottement dans l'anneau. L'excentricité conduit à une distribution asymétrique du débit, qui à son tour a un impact sur le gradient de pression global et l'efficacité du transport des fluides. Les résultats mettent en évidence la nécessité de tenir compte de l'excentricité dans la conception et l'exploitation des systèmes de puits de forage. L'étude fournit des informations pratiques sur l'optimisation des processus de forage et d'extraction, dans le but de minimiser les pertes de pression et d'améliorer l'efficacité opérationnelle. En améliorant la compréhension de la façon dont l'excentricité et d'autres paramètres influencent la dynamique de la pression, cette recherche contribue à des opérations de forage plus sûres et plus rentables.

الملخص:

تبحث هذه الأطروحة في تأثير ريولوجيا السوائل وتدفق الطور المتعدد على ديناميكيات الضغط والتدفق في أنظمة الآبار غير النيوتونية، مع التركيز بشكل خاص على العوامل التي تؤثر على فقدان الضغط. أحد المعايير الرئيسية التي تم تناولها في هذه الدراسة هو الانحراف، الذي يشير إلى الإزاحة بين جدار البئر وسلسلة الحفر. السوائل غير النيوتونية، التي تتميز بسلوك لزوجة معقد، تطرح تحديات فريدة في عمليات الآبار، لاسيما في الحفر والإنتاج وعمليات الإكمال. يتم تحليل المعايير الرئيسية مثل لزوجة السوائل، معدل القص، سرعة التدفق، هندسة الأنابيب، وخصوصًا الانحراف بشكل منهجي. تكشف النتائج أن الانحراف يؤثر بشكل كبير على فقدان الضغط من خلال تغيير أنماط التدفق وزيادة القوى الاحتكاكية داخل الفراغ الحلقي. يؤدي الانحراف إلى توزيع غير تُبرز النتائج الضرورة لأخذ الانحراف في .متماثل للتدفق، مما يؤثر بدوره على التدرج الضغط والكفاءة العامة لنقل السوائل الاعتبار عند تصميم وتشغيل أنظمة الآبار. توفر الدراسة رؤى عملية لتحسين عمليات الحفر والاستخراج، بهدف تقليل فقدان الضغط وتحسين الكفاءة التشغيلية. من خلال تعزيز الفهم لكيفية تأثير الانحراف والعوامل الأخرى على ديناميكيات الضغط، تُسهم هذه الدراسة في عمليات آبار أكثر أمانًا وفعالية من حيث التكلفة

Dedication

I have the great honor to dedicate this modest work: To myself, as a culmination of all the sleepless nights and sacrifices throughout my journey.

To the remarkable woman who has endured so much to shape me into who I am, who gives me hope to live, and the strength to pursue my dreams and succeed. To the one woman in my life, my beloved mother

To my dear father for his sacrifices in making my wishes come true, and for all his prayers that have provided me with support and encouragement.

To my dear sisters and my dear brothers, who have always supported me financially and emotionally at every moment, without expecting anything in return.

To my dear friends and all my closest friends

To all those who have wished me success and happiness

- Zouari Ahmed Souhaib -

Dedication

This thesis is dedicated to my beloved parents, whose endless love, support, and sacrifices have been the cornerstone of my journey. Mom and Dad, your unwavering belief in me has provided the strength and determination I needed to persevere. Your guidance, wisdom, and constant encouragement have been my guiding light.

To my brothers and sisters, who have been my pillars of support and my greatest cheerleaders. Your constant encouragement, understanding, and patience have been my rock through this challenging yet rewarding journey. Each of you has played an integral role in my life, providing the joy, comfort, and motivation I needed to succeed.

Mom and Dad, thank you for instilling in me the values of hard work, dedication, and the importance of education. Your sacrifices and love have not gone unnoticed, and I am forever grateful for everything you have done for me. You have taught me to dream big and to never give up, no matter how difficult the path may be.

To my brothers and sisters, thank you for always being there for me, for your endless support, and for believing in me even when I doubted myself. Your laughter, love, and encouragement have been my solace and my strength. I am blessed to have you all in my life.

This accomplishment is not mine alone; it is a testament to the love, support, and encouragement of my family. I am deeply grateful to each of you for being my rock and my inspiration. This thesis is dedicated to you, with all my love and gratitude.

- Si Hamdi Mohamed El-Amine -

Dedication

I dedicate this work with great love to my dear parents SLIMANI A. and KHALADI. F, for all their love, sacrifices, tenderness, support, and prayers throughout my studies.

To my dear brother Abderrahman and my dear sisters Yasmine and Zahira for their constant encouragement, and moral support, To my friend Tofahha O., to all my friends, especially my study partners Souhaib and Mohamed

To all my family, especially my grandmother KOUACH M. and my grandfather Mouloud, my golden gems KHALADI R. and SLIMANI F.

Special dedication to my aunt Dr. KHALADI R. who has a great merit in this work.

To everyone who holds a place in my heart May this work be the fulfillment of your sincere wishes, and the result of your unwavering support,

Thank you for always being there for me.

- SLIMANI ZIAD -

Table of contents

CHAPTER 2: PRESSURE AND FLOW DYNAMICS & PRESSURE-LOSS MODELING

Lists of figures

Lists of tables

NOMENCLATURE

A	cross-sectional area.
C_{vert}	cuttings concentration in the vertical section
D	diameter.
E	modulus of elasticity, (psi)
e	eccentricity, dimensionless
f:	friction factor.
I	moment of inertia of the drill pipe (inch),
k	consistency coefficient
n	flow behavior index (dimensionless)
Re	Reynolds number.
μ	fluid viscosity (cp)
μ_a	apparent viscosity
μ_p	plastic viscosity of the fluid in mPa.s (cp)
v	fluid velocity, m/s.
W	weight on bit, (Ib)
X	drill pipe horizontal projection, 1000 inches
τ:	shear stress (Pa)
γ:	shear rate (s^{-1})
θ_{600}	viscometer dial reading at 600rpm
θ_{300}	viscometer dial reading at 300rpm
τ_0	yield stress and the unit is lb /100ft2 or Pa
ϵ	equivalent sand-grain roughness.
ρ	density of the fluid, kg/m3;
δ	distance between centers of inner and outer pipes, L
θ	hole inclination angle, (degree)

General Introduction

Investigating the influence of fluid rheology and multiphase flow on pressure and flow dynamics within non-Newtonian wellbores presents a complex and fascinating exploration into the interplay between fluid characteristics and wellbore conditions.

Non-Newtonian fluids, unlike Newtonian fluids such as water or air, exhibit viscosity that varies with the applied stress or strain rate. This behavior introduces complexities in flow dynamics, as the viscosity can change with factors like shear rate, pressure, and temperature. Consequently, the flow behavior of non-Newtonian fluids is highly dependent on the specific rheological properties of the fluid, which can include shear-thinning, shear-thickening, viscoelasticity, or yield stress.

The combination of non-Newtonian fluid rheology and multiphase flow introduces intricate challenges in predicting and controlling pressure and flow dynamics. Understanding how these factors interact is crucial for optimizing processes, designing efficient systems, and mitigating risks in various industries and scientific domains. Advances in computational modeling, experimental techniques, and theoretical frameworks continue to enhance our understanding of these complex fluid dynamics, driving innovation and progress across diverse fields.

CHAPTER 1:

GENERALITY

1 Overview of Non-Newtonian Fluid rheology:

1.1 Definition:

The fluid viscosity of non-Newtonian fluids is a function of the shear stress, the current shear rate, and/or the shear history (Figs. 1 and 2). Thixotropic, rheopectic, visco-elasticity, shear thinning (pseudoplastic), shear thickening (dilatant), yield stress (viscoplastic), and thixotropic viscosity are examples of the macroscopic flow behaviors of drilling fluids. Depending on the way the fluid structure responds to the applied shear forces, different macroscopic flow behavior types can be present . The classical lubrication theory of Newtonian fluids developed by Reynolds **[1]**, is expanded to non-Newtonian fluids. **[2]**

1.1.1 Pseudo-plastic Fluid :

Shear thinning fluids, or pseudo-plastic fluids, typically have lower viscosities at increasing shear rates. The flow behavior index for pseudoplastic fluids (Figs. 1) is typically less than one, or $n < 1$. Plotting them on a log-log paper also shows a linear relationship between shear stress and shear rate. Emulsion paint is one example.

1.1.2 Dilatant :

Shear thickening dilatant fluids are less common in nature than shear thinning fluids. When the shear force is applied, dilatant fluids become exponentially more viscous; that is, their flow behavior index is more than one, or $n > 1$ (Fig. 1.1). Mechanisms in which the shear stress, communicated via the continuous media, orients or twists the suspended particles in opposition to the randomizing effects of Brownian motion have been linked to this non-Newtonian flow behavior **[3]**. As the shear rate rises, the apparent viscosity of the dilatant fluid also rises. The quicksand is a dilatant fluid example.

1.1.3 Visco-plastic or Yield Stress Fluid :

A visco-plastic fluid is a fluid that requires a finite shear stress, below which it will not flow. In other words, the fluids behave as rigid bodies at low stresses but flow as viscous fluids at high stresses. A common example is the tooth paste, in which the content will not flow out until a reasonable amount of stress is applied on the tubular container.

1.1.4 Thixotropy :

Thixotropy, also known as time-dependent pseudoplastic fluid behavior, is a time-dependent shear thinning property of a fluid (Fig. 1.2). According to **[4]** and **[5]**, it is a

reversible and time-dependent structural change in fluid flow behavior brought on by stress or strain under shear, which is then rebuilt by Brownian motion**[6]**. When a thinxotropic fluid is subjected to a sharp change in shear rate, it takes a finite amount of time to reach equilibrium viscosity. It is commonly believed to be the time-dependent reduction in fluid viscosity brought on by a measurable, finite, and reversible microstructure change in the fluid during shear. In other words, certain fluids or gels that are thick or viscous under static conditions will flow, that is, become thin and less viscous over time when agitated, stressed, shaken or sheared. Such fluids are called thixotropic fluids. Examples include: drilling mud **[7]**, clays, bentonite suspension, tomato ketchup and yogurt.

1.1.5 Rheopectic Fluid :

Rheopecty, also known as rheopexy, is the time-dependent rise in viscosity that occurs in a non-Newtonian fluid when the fluid experiences a gradual increase in shearing force, or stress. In other words, it is a timedependent dilatant fluid behaviour. Printer inks, gypsum pastes, and lubricants are a few instances of rheopectic fluids. (Fig.1. 2)

1.1.6 Visco-elastic Fluids :

A material's ability to display both viscous and elastic properties during deformation is known as viscoelasticity. When stress is applied, they resist shear flow and strain linearly with time. Visco-microstructure reacts to stress and strain either in a non-linear way, where the microstructure changes in response to the applied stresses and strains, but in a reversible way, or in a linear manner, where the microstructure does not change itself **[4]**. Polymeric fluid is a good illustration of a viscoelastic fluid.

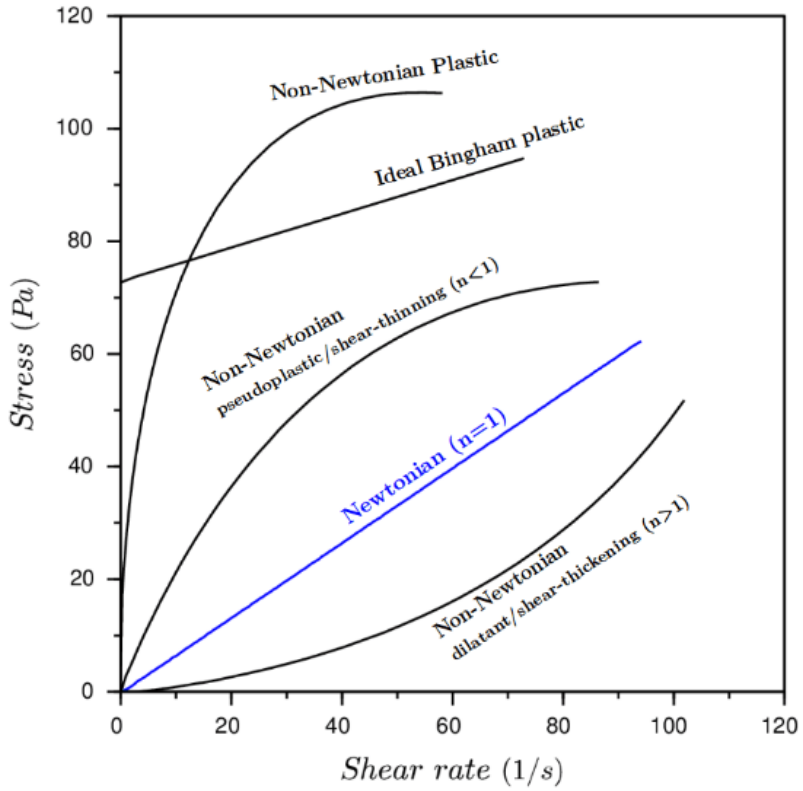

Figure 1. 1 - Shear Stress Versus Shear Rate for Thixotropic and Rheopectic Fluids

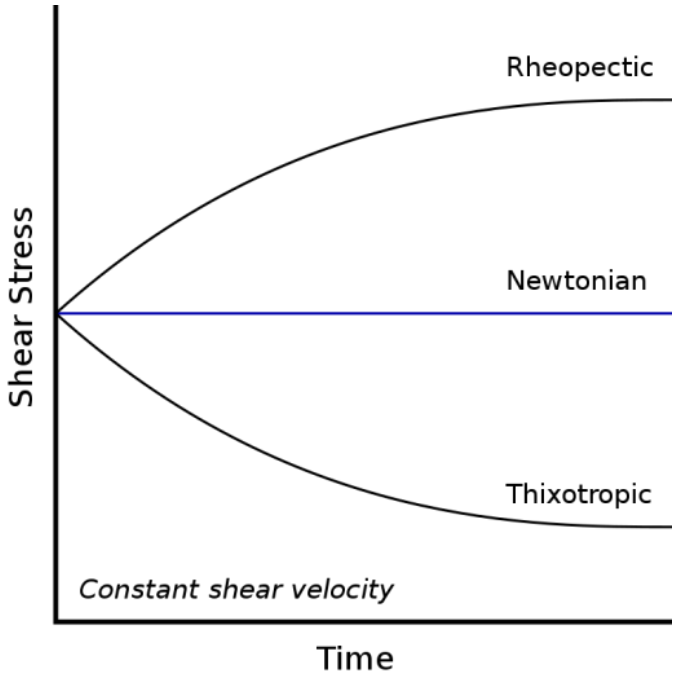

Figure 1. 2 - Shear Stress Versus Shear Rate for Thixotropic and Rheopectic Fluids

2 Rheology

2.1 Rheological Parameters of Drilling Fluids:

2.1.1 Fluid Viscosity

The viscosity of a fluid (μ) is defined as the degree of resistance to flow offered by the fluid. It can also be expressed as the resistance offered by the fluid to deformation when it is subjected to shear stress. Its mathematically quantified as the ratio of the shear stress (τ) to that of the shear rate (γ)

$$\mu = \frac{\tau}{\gamma} \qquad \text{Eq.1}$$

where,

μ: fluid viscosity

τ: shear stress

γ: shear rate

2.1.2 Shear Stress

This is the force that causes deformation of a material through mechanical slippage along a plane parallel to the material's surface. The force needed to transport a fluid through a material with a specific cross-sectional area is also known as viscosity. It is an external force acting on a material or surface parallel to the slope or plane in which it is located. In laminar flow, shear stress is the frictional drag that exists between individual laminae.

Mathematically,

$$\text{Shear stress } (\tau) = \frac{\text{force}}{\text{area}} \qquad \text{Eq.2}$$

It is expressed in N\m^2, (lb\100ft^2), Pascal or dynes\cm^2

2.1.3 Shear Strain:

It is a dimensionless quantity that characterizes the deformation of a material due to stress.

2.1.4 Shear Rate

This is defined as the rate at which one layer of fluid changes velocity when it passes over another, divided by the distance between the two. The unit is sec-1 (reciprocal seconds).

If the shear rate is specified in revolution per minute (RPM), it can be translated into sec-1 by using :

$$\gamma = 1.703*RPM \qquad \text{Eq.3}$$

The relationship between shear rate and shear stress for a fluid defines how the fluid will flow **[8]**.

2.1.5 Plastic Viscosity

Plastic viscosity is the resistance of a fluid to flow due to mechanical friction between suspended solid particles and the liquid phase. It refers to a fluid's viscosity at a high shear rate.

In drilling, plastic viscosity is sensitive to solid concentration, indicating the need for dilution. It is concerned with the drilling fluid's ability to transport rock cuttings to the surface, particularly in bigger hole sizes when the annulus velocity generated by the pump is relatively low **[9,10]**. The viscosity must be high enough to allow sand and cuttings to settle out and entrained gas to escape to the surface.

A moderate plastic viscosity is required for enhanced bit energy, increased rate of penetration, greater flow in the annulus for hole cleaning, low wear and tear, and reduced fuel consumption by circulating system equipment.

However, too little plastic viscosity causes cuttings to fall out of the slurry and deposit behind the drill head, resulting in drilling failure.

A very high plastic viscosity can be reduced by adding water (dilution) or mechanically separating excess solids because too high viscosity increases pump pressure, magnifying the swab or surge effect during tripping operation, and limiting flow properties, which reduces penetration rates. Similarly, a low viscosity mud can be improved by adding a viscosifier, such as organophilic clay for oil-based mud or bentonite for water-based mud. **[10]**

Plastic viscosity of a fluid is defined as the difference between the 600rpm and the 300rpm viscometer dial readings and it is usually expressed in centipoise (cp) or milliPascal seconds (mPa.s).

Mathematically,

$$\mu_p = \theta_{600} - \theta_{300} \qquad \text{Eq.4}$$

where,

μ_p: plastic viscosity

θ_{600}: viscometer dial reading at 600rpm

θ_{300}: viscometer dial reading at 300rpm

Drilling fluid plastic viscosity is principally determined by the following factors:

- Solid concentration.
- Size and shape of the solid particles found in mud.
- Viscosity of the liquid phase.
- The presence of some long chain polymers.
- The oil-to-water or synthetic-to-water ratio in invert-emulsion fluids.
- The type of emulsifier used in invert emulsion fluids.

2.1.6 Apparent Viscosity

This is the viscosity of a drilling fluid with a constant shear rate and temperature. It is calculated using the fluid's plastic viscosity and yield point and is represented in centipoise (cp). To maximize rate of penetration, it is crucial to understand the apparent viscosity at high shear rates in the bit nozzles **[11]**. Apparent viscosity is sometimes called effective viscosity.

Apparent viscosity is expressed mathematically by :

$$\mu_a = \frac{\theta_{600}}{2} \qquad \text{Eq.5}$$

where,

μ_a : apparent viscosity

θ_{600}: viscometer dial reading at 600rpm

2.1.7 Yield Point

The yield point represents the annulus's low shear rates and has a significant impact on cuttings carrying capacity and annular frictional pressure drop. It measures the electrochemical or attractive forces that exist between particles in a fluid under flow circumstances. It is the resistance to beginning flow or the stress necessary to move a liquid. These forces are caused by negative and positive charges present on or near the particle surfaces. Yield point is sensitive to the electrochemical environment, indicating that mud should be chemically treated. The yield point will fall as the attraction forces are lessened through chemical treatment. Reducing

the yield point will also reduce the perceived viscosity. It is expressed in pounds per 100 square feet (lb\100ft^2).

Mathematically, it is defined as the difference between the 300rpm dial reading and the plastic viscosity.

Yield point can be expressed Mathematically as:

$$\tau_0 = \theta_{300} - \mu_P \qquad \text{Eq.6}$$

where,

τ_0: yield point (lb/100ft)

θ_{300}: viscometer dial reading at 300rpm

μ_p: plastic viscosity

Yield point is often influenced by changes in the surface characteristics of the fluid particles, volume concentration of the solids, and electrical environment of these solids (ion concentration and kinds in the fluid phase of the fluid) **[12]**.
A yield point of 3 to 30 lbm/100ft2 is considered acceptable for unweighted clay/water based mud in order to improve the mud's ability to carry cuttings to the surface while not increasing the frictional pressure drop in the annulus sufficiently to cause formation fracture.
The ratio (YP/PV) can be used to quantify the shear thinning behavior of drilling fluids, with higher ratios indicating greater shear thinning.

2.1.8 Gel-Strength

Gel strength describes how the mud behaves when mud pumping is halted. The gel strength of drilling fluids is crucial for suspending drill solids and weighing materials during tripping operations. It has a significant impact on the pressure necessary to break circulation after a circular trip, as well as the size of swab and surge pressure.

It is defined as the shear stress of drilling mud measured at low shear rates after it has been static for a certain amount of time. The shearing tension required to commence a finite rate of shear. While the yield point and plastic viscosity are related to the properties of the mud while it is flowing, the gel strength evaluates the properties of the mud when it is stationary. Drilling fluid is thixotropic. This means that when they're not moving, they form a gelled structure. When the pump is turned on, the gel breaks up and the mud returns to liquid form. These measurements are typically taken and reported as beginning gel strength (0 quiescent

time) and final gel strength (10 quiescent time). The study focuses on two gel strengths: 10 seconds and 10 minutes. The 10 second gel strength is the highest dial deflection seen when the cup is twisted by hand immediately after the flow stops. The maximum dial deflection obtained when the viscometer is turned on after a ten-minute static period is known as the 10-minute gel strength.

Excessive gel necessitates the employment of a high pump pressure to transfer the fluid, which might cause formation damage. The unit is (pounds per square foot). To solve an excessive gel strength or yield point, add chemical thinners (deflocculants) such as phosphates, tannins, lignins, and lignosulfonates to the drilling mud.

3 Overview of Relevant Rheological Models

3.1 Newtonian Model

The Newtonian model assumes that shear stress(τ) is directly proportional to shear rate(γ), with the fluid viscosity serving as the proportionality constant, as illustrated in Figure 1.3. Shear stress can be defined mathematically as:

$$\tau = \mu * \gamma \qquad \text{Eq.7}$$

where,

τ: shear stress

μ: fluid viscosity

γ: shear rate

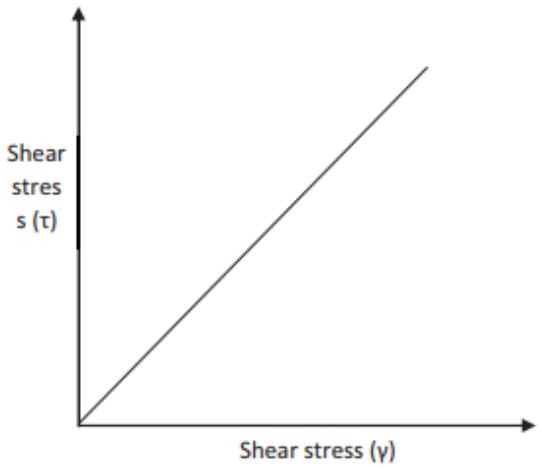

Figure 1. 3 - Viscosity Profile of Newtonian Fluid

3.2 Non-Newtonian Model

The fluid viscosity is not constant but a function of the shear stress and/or the prevailing shear rate or shear history as shown in Fig 1.4.

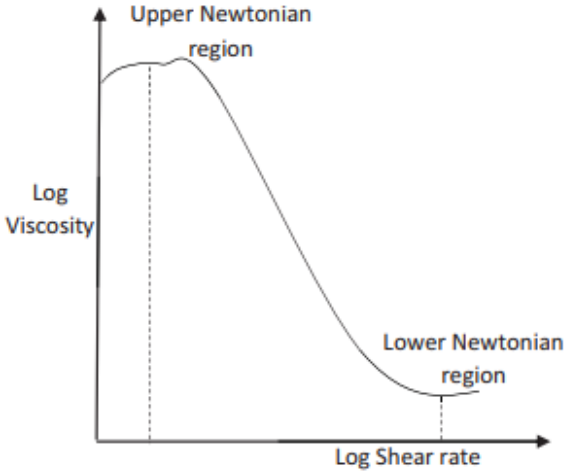

Figure 1. 4 - Viscosity Profile of non-Newtonian Fluid

For non-Newtonian models, there is frequently an area at both low and high shear rates where the viscosity is independent or substantially independent of shear rate, and a part in the middle that exhibits strong shear rate dependency **[13]**.

3.2.1 Bingham Plastic Model

The Bingham plastic model is a two-parameter model commonly used in the drilling fluid industry to describe the flow properties of various types of muds. It is mathematically described by **Equation 8**. Bingham Plastic fluids have plastic viscosity and yield stress that are independent of shear rate **[14]**. The shear stressshear strain relationship is shown in Fig 1.5.

$$\tau = \tau_0 + \mu_p \gamma \qquad \text{Eq.8}$$

where,

τ: shear stress

τ_0: yield stress and the unit is lb /100ft2 or Pa

μ_p: plastic viscosity of the fluid in mPa.s (cp)

γ: shear rate

Bingham plastic fluid requires a finite stress to initiate a flow

At low stress levels, Bingham plastic fluid behaves rigidly, but at higher strains, it begins to flow like a viscous fluid. Toothpaste is a common example of a fluid. The model is used to explain a fluid that requires a finite stress to commence a flow (yield point) and subsequently exhibits a constant viscosity with increasing shear rate (plastic viscosity).

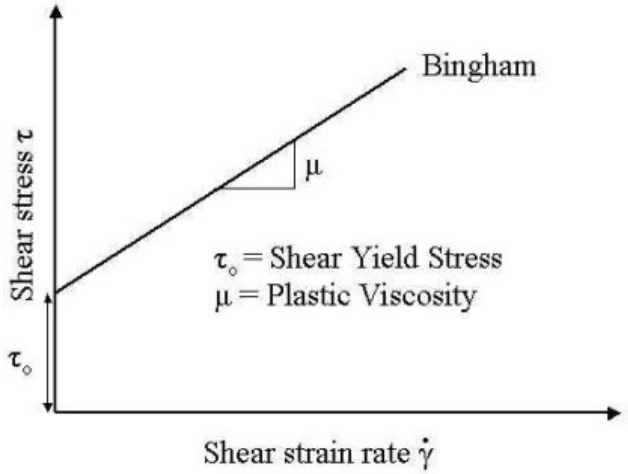

Figure 1. 5 - Bingham plastic Model shear-stress versus shear-strain Relationship

3.2.2 Power Law Rheological Model :

The power law model [Fig 1.6] is expressed as:

$$\tau = k\gamma^n \qquad \text{Eq.9}$$

where,

τ: shear stress

k: consistency coefficient

γ: shear rate

n: fluid flow behavior index

Where n is the fluid flow behavior index, which indicates the tendency of a fluid to shear thin and is dimensionless, and k is the consistency coefficient, which serves as the viscosity index of the system, and the unit is lb/100ft2, which can be converted to Pascal units by multiplying by a factor of 0.511 **[15]**. The power law model gives a better information in the low shear rate condition but has drawbacks in high shear rate conditions.

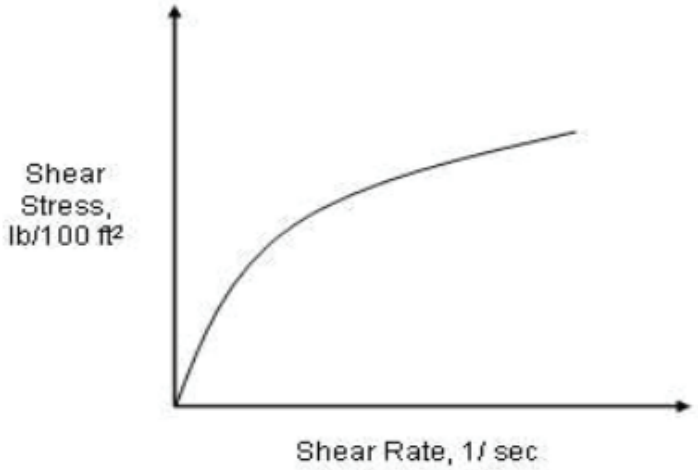

Figure 1. 6 - Power Law Model Shear-stress versus Shear-strain Relationship

3.2.3 Herschel-Bulkley Rheological Model :

The Hershel-Buckley Model [Fig 1.8] is an extension of the Bingham Plastic Model that incorporates shear rate dependency. It is a three-parameter rheological model that describes the flow behaviour of drilling fluid. The model presented by Herschel and Bulkley **[16]**

is given by Eq :

$$\tau = \tau_y + k\gamma^n \qquad \text{Eq.10}$$

where,

τ: shear stress (Pa)

γ: shear rate (s^{-1})

n: flow behaviour index (dimensionless)

k: HRBM consistency index in (Pa)

τ_y: HBRM yield stress (Pa).

If the yield stress of a fluid sample is known from an independent experiment, the parameters k and n can be determined by linearizing Eq.10 as follows:

$$\text{Log}\,(\tau-\tau_y) = \log k + n\log(\gamma) \qquad \text{Eq.11}$$

And a plot of log $(\tau-\tau_y)$ versus log (γ) will result in a straight line with intercept log k and slope n respectively as shown in Fig.1.7.

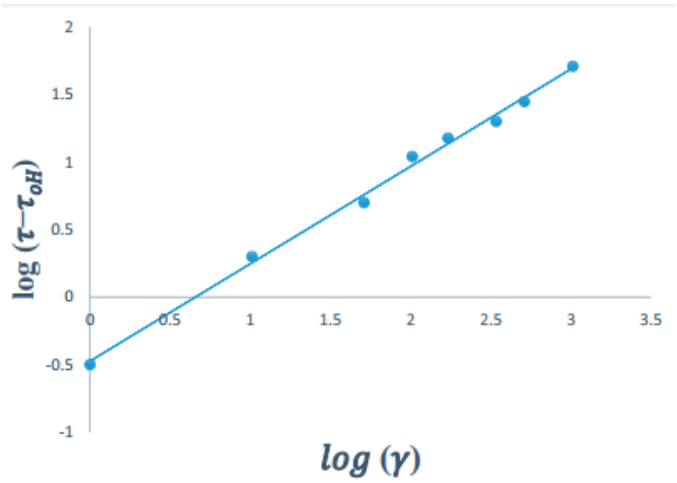

Figure 1. 7 - Herschel-Bulkley Rheological Model Logarithmic Graphical Representation

The Bingham Plastic model cannot accurately represent fluids with a stress- or strain-dependent yield point and viscosity. The Herschel-Bulkley model addresses this issue by replacing the plastic viscosity term in the Bingham Plastic model with a power law expression. However, the concept of yield stress has been questioned since a fluid can deform minutely at stress levels lower than the yield stress.

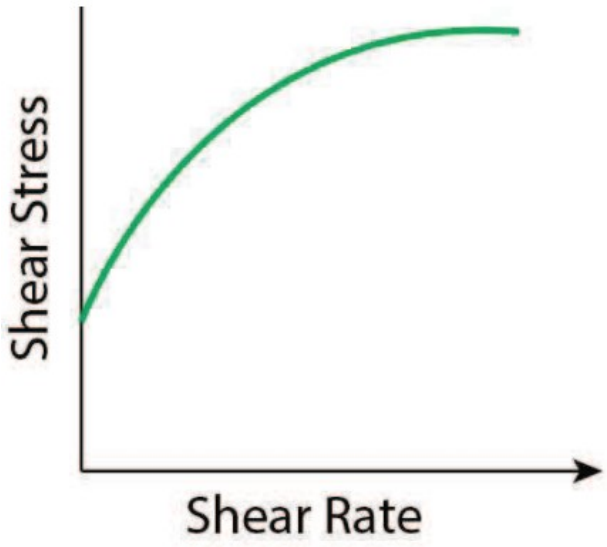

Figure 1. 8 - Herschel Bulkley Model shear-stress versus Shear-strain Relationship

4 Multiphase Flow in Wellbores

4.1 Cement

Imagine cement as the dense, solid-like phase in a multiphase flow. It's the heavyweight that settles to form a strong, impermeable layer. As it flows through the wellbore, it starts as a thick, viscous fluid but rapidly transitions into a solid phase, creating a sturdy barrier. Its properties are crucial; if it's too thick, it won't flow properly, but if it's too thin, it won't set correctly. The cement phase is all about finding that balance to ensure the wellbore is sealed and stabilized.

4.2 Spacer

The spacer fluid can be thought of as the intermediate phase that bridges the gap between the drilling mud and the cement. In the multiphase flow analogy, it acts like a buffer, ensuring a clean transition. The spacer's role is to make sure that the cement and drilling mud don't mix, which could compromise the wellbore's integrity. It has to be compatible with both the mud and the cement, maintaining its own distinct phase while effectively cleaning and conditioning the wellbore for the cement to follow.

4.3 Mud

Drilling mud is the initial, continuous phase in this multiphase flow system. It's the fluid that keeps everything moving smoothly, carrying cuttings away from the drill bit and stabilizing the wellbore walls. When it’s time for cementing, the mud needs to be displaced efficiently by the spacer. The challenge here is to manage the flow properties of the mud so that it can be effectively replaced without leaving any residues that could interfere with the cement setting process.

In a multiphase flow scenario, each phase—mud, spacer, and cement—must be meticulously managed to ensure that they flow in harmony, each doing their part to maintain the wellbore's integrity. The interactions between these phases are dynamic and complex, requiring precise control and understanding of their individual flow characteristics to achieve a successful cementing job.

CHAPTER 2:

PRESSURE AND FLOW DYNAMICS & PRESSURE-LOSS MODELING

1 Flow Dynamics

1.1 Flow Regimes

Fluid flow has three different regimes: turbulent, laminar, and transitional. The flow characteristics in each fluid flow regime are simple to comprehend, but they can be challenging to replicate and will necessitate specific numerical approaches in general.

1.1.1 Laminar Flow

When a fluid flows in the laminar domain, its flow behavior is simple to see and understand. Flow is fully propelled by external factors, which are typically gravity and driving pressure. Laminar flow is commonly described as happening solely in incompressible inviscid fluids, which is erroneous. The Euler equations can be used to predict flow behavior in inviscid, incompressible flows, but the generic Navier-Stokes equations are utilized in other flow conditions where turbulence may occur or the fluid is compressible.

In laminar flow, the fluid flows smoothly and linearly along the system's boundary. For example, the flow pattern in a pipe is relatively linear and does not exhibit significant changes. When the Reynolds number for the flow increases, the fluid flow characteristic shifts from laminar to turbulent.

1.1.2 Turbulent Flow

The turbulent flow regime is at the opposite end of the flow spectrum, corresponding to extremely fast flow rates. Turbulence is one of the most mathematically complex fields of fluid dynamics, necessitating numerical approaches and specialized models to investigate flow behavior. When turbulence occurs, fluid flow becomes convective (vortical), forming in the boundary layer and expanding along the flow direction. Turbulent flow behavior is not always random, but statistical methods can be used to estimate the level of turbulence.

Instead of being random, the exact trajectory of turbulent flow is deterministic and predictable, however it is extremely sensitive to initial and boundary circumstances. Furthermore, ostensibly laminar flow can quickly become turbulent with minor changes in system parameters (direction, density, flow rate, etc.). An outstanding example is in aerodynamics, where airflow over an airfoil can become turbulent as the angle of attack varies, even if other flow characteristics remain constant.

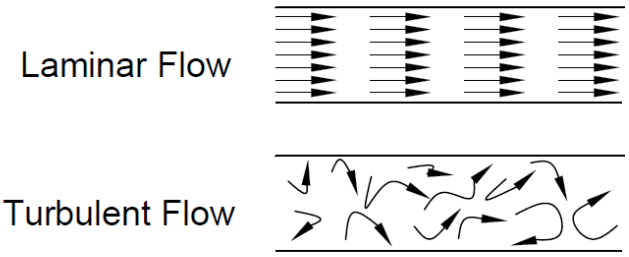

Figure 2. 1 - Laminar and turbulent flow

1.1.3 Transition Region

A transition area is a range of Reynolds number values in which the flow behavior begins to shift from laminar to turbulent. This should emphasize that there is no clear distinction between the laminar and turbulent regimes; the normal behavior observed in turbulent flow finally takes precedence at high Reynolds numbers. The precise range of Reynolds numbers is system- and fluid-specific, and even very comparable systems may have quite different Reynolds number values beyond which turbulence takes over.

The fundamental physics that causes a fluid to become turbulent rather than laminar as a function of Reynolds number is still being investigated. As a result, numerous models have been constructed in an attempt to represent and understand the mechanism driving the transition from laminar to turbulent flow.

2 Pressure Dynamics

2.1 Importance in Wellbore Systems

Pressure dynamics play a significant role in wellbore systems, which are used in the exploration and production of oil and gas. Understanding and managing pressure dynamics in wellbores is crucial for the following reasons:

- **Well Control and Safety:** Pressure dynamics in wellbores are intimately linked to well control and safety. Maintaining good pressure management is critical to avoiding blowouts, which occur when the formation pressure exceeds the hydrostatic pressure of the drilling fluid. By monitoring and managing pressure dynamics, operators can avoid uncontrolled escapes of oil, gas, or drilling fluids, assuring the safety of personnel and equipment.

- **Drilling Operations:** Pressure dynamics are crucial during the drilling process. The drilling fluid, or mud, is pumped down the drill pipe, through the bit, and back to the surface. The mud's pressure helps manage wellbore stability, prevent formation damage, and transport cuttings to the surface. Understanding pressure dynamics enables drillers to adjust drilling parameters such as mud weight and flow rate, resulting in efficient and safe drilling.
- **Formation Evaluation:** Pressure dynamics in wellbores reveal important information about the properties of subterranean formations. Geoscientists can calculate formation parameters like permeability, porosity, and fluid content by evaluating pressure data collected during drilling or well testing. This information is critical for reservoir characterization and estimating the well's prospective productivity.
- **Wellbore Integrity:** Pressure dynamics can have an impact on the wellbore's overall integrity. Pressure changes, such as surges or swabbing effects, can cause wellbore instability, mud loss, and formation damage. Understanding pressure dynamics allows engineers to design appropriate casing and cementing programs that ensure wellbore integrity throughout the well's life.

2.2 Factors Affecting Pressure Dynamics

Pressure dynamics can be influenced by several factors that affect how pressure changes over time. These factors include:

2.2.1 Flow Rate

The rate at which fluid moves through a system can influence pressure dynamics. Higher flow rates can result in more pressure decrease owing to frictional losses, whereas lower flow rates can cause pressure building. Changes in flow rate can create pressure fluctuations, affecting the system's overall dynamics.

2.2.2 Fluid Properties

The qualities of the fluid that flows through a system have a substantial impact on pressure dynamics. Variables like viscosity, density, and compressibility can influence how pressure varies as the fluid flows through the system. For example, extremely viscous fluids may experience greater pressure drops than less viscous fluids at the same flow rate.

2.2.3 Pipe Diameter and Length

The pipe's dimensions, including diameter and length, might affect pressure dynamics. Smaller pipe sizes can cause a larger pressure drop due to increased frictional losses, whereas longer pipes can contribute to a steady pressure reduction. Pressure dynamics are strongly influenced by the pipe system's geometry.

2.2.4 Fluid Density and Viscosity

The density and viscosity of a fluid can influence pressure dynamics. Higher fluid densities can result in higher pressure drops, whilst higher viscosities can contribute to increased friction losses. These qualities influence the fluid's flow behaviour and, as a result, pressure dynamics.

2.2.5 Temperature

Temperature changes can affect pressure dynamics. As a fluid's temperature varies, its density and viscosity change, influencing pressure drop and flow behaviour. Temperature changes can induce pressure fluctuations and change the overall dynamics of the system.

2.2.6 Effect of Tool Joint Restrictions

The tool joint is a necessary part to extend the drillpipe. These components are fabricated separately from the pipe body and welded onto the pipe at a manufacturing facility. The tool joint provide high-strength, high pressure threaded connections that are sufficiently robust to survive the heavy duty and extreme loads at the rig. Tool joints have smaller inside diameters than the drillpipe body and larger outside diameter.

The presence of tool joints restricts flow in pipes with contraction and expansion the fluid as it enters and departs the tool joint. The pressure loss induced by entering the tool joint is negligible when compared to the exit losses. Tool joints, on the other hand, have a larger outside diameter which changes the annulus geometry between the drillpipe and the casing/hole, causing severe turbulence and fluid acceleration, resulting in an increased viscous dissipation and pressure losses. This effect is anticipated to be limited due to the annulus's low fluid velocity.

2.2.7 Effect of Drillstring Rotation

Pipe rotation is mandatory to rotary drilling as it is responsible for many functions. The drilling community believes that pipe rotation improves hole cleaning especially in horizontal and heavily deviated wellbores. There has been a lack of stidies on how pipe rotation affects

frictional pressure loss. Recent researches indicates that drillstring rotation has a considerable impact on pressure loss, especially for slim hole, extended reach, horizontal and highly deviated drilling applications. The effect of drillpipe rotation can vary significantly depending on rotation speed, fluid characteristics, flow regimes, diameter ratio, and eccentricity. Even at small rates, drillpipe rotation produces unstable flow and accelerates the transition from laminar to turbulent flow.

2.2.8 Effect of Drillstring Eccentricity

The annular frictional pressure losses of vertical or near vertical well sections differ from the highly inclined and horizontal wellbores. This is because of natural tendency of the drillstring to lay down on the low side of the wellbore due to gravity. This configuration forms eccentric annulus and generally referred to as drillstring eccentricity. Hence, the assumption of a concentric annulus is often not realistic, particularly, for horizontal and highly deviated wellbores. Moreover, the drillstring is elastic and has the possibility to wobble in the hole during rotation. It can be positioned differently in the wellbore cross section at different depths, depending on inclination and hook load **[17].** The pressure losses depend on the annulus eccentricity. Moving the drillstring to the wall of the wellbore creates a bigger flow channel in the annulus, changing the direction and acceleration of the annular flow and reduces the frictional pressure losses significantly.

Many experimental studies on hydraulics of eccentric annuli have been conducted. Their results show that pressure loss decreases as eccentricity increases. Pressure losses ranging from 18 to 40% lower than those of the concentric annulus were recorded. Eccentricity can minimize annular pressure losses by up to 40%, but dependency on fluid rheology and diameter ratio is less noticeable

2.2.9 Effect of pipe roughness

The effect of pipe roughness can be neglected under laminar flow condition but is significant in turbulent flow. Friction losses in rough pipelines are greater for both Newtonian and non-Newtonian fluids. However, due to the chaotic character and eddies of turbulent flow, it is extremely difficult to develop an exact mathematical method for calculating pressure losses. As a result, the equation for the friction factor must be simplified. The Blasius equation is one of the most common.

2.2.10 Effect of Cuttings Accumulations

Cuttings are generated by the bit are transported by the drilling fluid along the annulus. This affect the drilling fluid density and causes greater annular pressure losses than calculated. Furthermore, solid content increases the PV of BP fluids which included in pressure loss equations for BP fluids. Greater rate of penetrations, lower carrying capacity of the mud and inefficient solid control resulted in a higher concentration of these solids in the annulus and a greater effect on mud density and rheology. Cuttings accumulation are dominant at highly deviated wellbores. These cuttings are found as stationary or moving beds at the lower side of the wellbore.

Cuttings bedding causes a reduction in hydraulic diameter and flow area and increases the friction pressure loss. Therefore, in real drilling conditions the annular pressure loss will be affected by cuttings content as well as the other factors.

Usually, equivalent circulation densities (ECD) are estimated using the hydrostatic pressure and frictional pressure drop in the annulus, but the cuttings concentration is not taken into account. This could lead to underestimation of ECD values. Correct ECD is anticipated if cuttings concentrations and slip velocity of cuttings are both taken into consideration, especially for vertical and near vertical annuli.

2.2.11 External Factors

Changes in ambient temperature, elevation, or atmospheric pressure can all alter pressure dynamics. These factors can have an impact on overall pressure in the system and should be taken into account while assessing pressure behavior

Understanding these factors and their influence on pressure dynamics is important for designing, operating, and troubleshooting fluid systems. Accurate modelling, monitoring, and control of these factors can help ensure safe and efficient operation while maintaining desired pressure conditions

3 Pressure-loss modeling

3.1 Principle

The goal of this subclause is to give methods and equations for calculating frictional pressure losses and hydrostatic pressures as they pass through the various components of a drilling well's circulating system. The data is useful for hydraulics analysis, planning, and

optimization. It is also excellent for simulating specialized well-construction processes including well control, cementing, tripping, and casing runs. The equations in this subclause apply to water, oil, and synthetic-based fluids, but not to air/gas, foam, or other aerated or extremely compressible fluids.

3.2 Basic relationships

Pressures in the circulating system are defined by fundamental relationships between standpipe (pump) pressure and bottomhole pressure, which are valid in both static and dynamic settings.

Pump pressure (P_p) is the sum of frictional pressure losses, surface back pressure, and the hydrostatic pressure difference between the annulus and drillstring.

$$P_P = P_{SC} + P_{ds} + P_{dt} + P_b + P_a + P_{cl} + P_c + P_{ha} - P_{hd} \quad \text{Eq.12}$$

The pressure at the bottom of the well (P_{bh}) is the total of annular frictional pressure losses, surface back pressure, and annular hydrostatic pressure.

$$P_{bh} = P_a + P_{cl} + P_c + P_{ha} \quad \text{Eq.13}$$

3.2.1 Hydrostatic pressure

Hydrostatic pressure is determined by the true vertical depth D_v and the density profile of the drilling fluid column within the well. The volume percentage of drilled cuttings can be used to calculate the effective annular hydrostatic pressure. The method for calculating the average cuttings concentration (c) and cuttings specific gravity ρ_c

3.2.1.1 Hydrostatic pressure in conventional wells

For conventional wells, average density in the drilling fluid column can be approximated by the drilling fluid density measured at the surface ρ_s .

- **Pipe:**

$$P_{hd} = 0.052 * \rho_s * D_v \quad \text{Eq.14}$$

- **Annulus without cuttings:**

$$P_{ha} = 0.052 * \rho_s * D_v \quad \text{Eq.15}$$

- **Annulus with cuttings:**

$$P_{ha} = 0.052 * [(1- c)\ \rho_s + 8.345\ c\ \rho_s]* D_v \quad \text{Eq.16}$$

3.2.1.2 Hydrostatic pressure in HTHP and deepwater wells:

The density profile in high-pressure and extreme-temperature (hot and cold) wells is greatly influenced by temperature and pressure. The accurate hydrostatic pressures in the drillstring and annulus (P_{hd} and P_{ha}, respectively) in these sorts of wells are computed using equivalent static densities ESD_p and ESD_a specified at the true vertical depth of interest D_v.

- **Pipe:**

$$P_{hd} = 0.052 * ESD_p * D_v \quad \text{Eq.17}$$

- **Annulus without cuttings:**

$$P_{hd} = 0.052 * ESD_a * D_v \quad \text{Eq.18}$$

- **Annulus with cuttings:**

$$P_{ha} = 0.052 * [(1- c)\, ESD_a + 8.345\, c\, \rho_s\,]* D_v \quad \text{Eq.19}$$

3.3 Surface-connection pressure loss:

Pressure loss at surface connections P_{sc} varies with pipe shape, surface drilling fluid density ρ_s, and flow rate Q. Surface-connection piping is commonly categorized into five broad scenarios, and the pressure loss is estimated using the appropriate proportionality constant Csc from Table 1 .

$$P_{sc} = C_{sc} * \rho_s * \left(\frac{Q}{100}\right)^{1.86} \quad \text{Eq.20}$$

Table 1 - C_{sc} for surface-connection cases

Case	Standpipe	Hose	Swivel	Kelly	C_{sc}
1	40 ft x 3.0-in ID	45 ft x 2.0-in ID	4 ft x 2.0-in ID	40 ft x 2.25-in ID	1.00
2	40 ft x 3.5-in ID	55 ft x 2.5-in ID	5 ft x 2.5-in ID	40 ft x 3.25-in ID	0.36
3	45 ft x 4.0-in ID	55 ft x 3.0-in ID	5 ft x 2.5-in ID	40 ft x 3.25-in ID	0.22
4	45 ft x 4.0-in ID	55 ft x 3.0-in ID	6 ft x 3.0-in ID	40 ft x 4.00-in ID	0.15
5	100 ft x 5.0-in ID	85 ft x 3.5-in ID	22 ft x 3.5-in ID		0.15

3.4 Drillstring and annular frictional pressure loss

3.4.1 Principle

Flow rate, flow regime, rheological characteristics, and conduit shape are some of the important parameters that influence frictional pressure losses in the drillstring and annulus **[18,19,20].** The sensitivity of drilling fluid density and rheological properties to downhole temperatures and pressures complicates the process of modeling these pressures, which is complex in and of itself for Herschel-Bulkley fluids.

3.4.2 Section lengths for pressure-loss calculations

To incorporate downhole conditions, an efficient way is to subdivide the drillstring and annulus into short segments (or cells) of length L, similar to how the density profile is numerically integrated. For the most part, the equations and parameter values stated in this subclause apply to these specific cells. Geometric sections or casing intervals, which are often employed in conventional wells, can also be used in critical wells; however, the various parameters must be adequately averaged throughout each segment length.

3.4.3 Fluid velocity

Average (bulk) velocities V_p and V_a are inversely proportional to the cross-sectional area of the respective fluid conduit.

- Pipe:

$$\mathrm{Vp} = \frac{24.51Q}{d_i^2} \quad \text{Eq.21}$$

- Annulus:

$$\mathrm{Va} = \frac{24.51Q}{d_h^2 - d_p^2} \quad \text{Eq.22}$$

Riser Booster Pumps

Booster pumps are frequently employed in deepwater drilling to enhance riser flow and aid in hole cleaning operations. In these instances, the flow rate in the riser/drillstring annulus should equal the sum of the conventional and booster flow rates.

3.4.4 Hydraulic diameter

The hydraulic-diameter concept is used to compare fluid behavior in an annulus to that of a circular pipe. The annular hydraulic diameter dhyd can be expressed in a variety of ways

[21], but the most common is based on the ratio of cross-sectional area to wetted perimeter of the annular section. The hydraulic diameter for pipe flow is equal to the internal diameter d_i.

- Pipe:

$$d_{hyd} = d_i \qquad \text{Eq.23}$$

- Annulus:

$$d_{hyd} = d_h - d_p \qquad \text{Eq.24}$$

3.4.5 Rheological parameters

Rheological parameters for pressure-loss models are obtained using field and HTHP laboratory viscometers. Adjust surface-measured PV, YP, and τ_y values for downhole temperatures and pressures in each well segment before calculating n and k.

3.4.5.1 Bingham Plastic model parameters

The Bingham plastic model discusses fluids that are time-independent. It is a two-parameter rheological model that is widely applied in the drilling business. To commence flow in Bingham plastic fluids, an initial stress is necessary. The modeled shear stresses can be estimated using the equations below.

$$\tau = \mu_p \gamma + \tau_y$$

$$\mu_p = \theta_{600} - \theta_{300}$$

$$\tau_y = \theta_{300} - \mu_p$$

Where:

μ_p = Plastic viscosity, cp;

τ_y = Yield point.

3.4.5.2 Power-law model parameters

Several complex interactions for Herschel-Bulkley fluids are difficult, if not impossible, to analytically analyze. Under certain situations, Herschel-Bulkley fluids can be treated as generalized power-law fluids with parameters n_p and k_p. The Herschel-Bulkley flow equation is assumed to have a log-log slope similar to the power-law flow behavior index (n_p) at high shear rates.

$$n_P = 3.32\log_{10}\left(\frac{2PV+YP}{PV+YP}\right) \quad \text{Eq.25}$$

$$k_p = \frac{PV+YP}{511^{np}} \quad \text{Eq.26}$$

3.4.5.3 Herschel-Bulkley model parameters

To calculate Herschel-Bulkley parameters n and k in each downhole section, use the standard oilfield rheological parameters PV, YP, and τ_y. The τ_y /YP ratio R helps define rheological behavior (R = 0 for power-law, R = 1 for Bingham-plastic, and 0 < R < 1 for Herschel-Bulkley fluids).

$$n = 3.32\log_{10}\left(\frac{2PV+YP-\tau_y}{PV+YP-\tau_y}\right) \quad \text{Eq.27}$$

$$k = \frac{PV+YP-\tau_y}{511^{n}} \quad \text{Eq.28}$$

$$R = \frac{\tau_y}{YP} \quad \text{(for YP > 0)} \quad \text{Eq.29}$$

3.4.6 Shear-rate geometry correction factors

To compute pressure loss, translate the Newtonian (or "nominal") shear rate γ to the shear rate at the wall, γ_w. This is performed by employing correction factors that account for the geometry of the flow conduit (pipe or annulus) and oilfield viscometers to measure rheological parameters.**[22]** The appropriate corrections can be bundled into a single factor, G.

3.4.6.1 Well geometry shear-rate correction

Shear-rate correction for well geometry B_a also depends on the rheological parameter n. Using a geometry factor α simplifies the calculation for flow in pipes and annuli. To simplify without sacrificing accuracy, the annulus can be considered as an analogous slot (α = 1).

$$B_a = \left[\frac{(3-\alpha)n+1}{(4-\alpha)n}\right]\left[1+\frac{\alpha}{2}\right] \quad \text{Eq.30}$$

where

α = 0 is the geometry factor in the pipe

α = 1 is the geometry factor in the annulus

3.4.6.2 Field viscometer shear-rate correction

Unfortunately, there are no closed analytical solutions for Herschel-Bulkley fluids, and complicated numerical approaches are erroneous at extremely low shear rates. In practice, we can assume that the viscometer correction B_x is around 1. If exact solutions for power-law fluids are required, B_x can be utilized instead **[23]**. For the conventional bob/sleeve combination, B_x for power-law fluids ranges from 1.0 (n_p = 1.0) to 1.1569 (n_p = 0.3).

$$B_x = \left[\frac{x^{\frac{2}{n_p}}}{n_p x^2}\right]\left[\frac{x^2-1}{x^{\frac{2}{n_p}}-1}\right] \approx 1 \qquad \text{Eq.31}$$

where

x = 1.0678 in the standard bob/sleeve combination R1B1

3.4.6.3 Combined geometry shear-rate correction factor

The well geometry and viscometer shear-rate correction factors can be combined to form a single factor G, which is used to convert nominal shear rate to wall shear rate. In many circumstances, it is reasonable to assume $B_x \approx 1$.

$$G = \frac{B_a}{B_x} \qquad \text{Eq.32}$$

3.4.7 Shear rate at the wall

Shear rate on the wall to compute shear stress at the wall, multiply the nominal shear rate by the geometry factor G (γ_w). This equation is valid for pipes and annuli for appropriate fluid velocity V and hydraulic diameter d_{hyd}.

$$\gamma_w = \frac{1.6GV}{d_{hyd}} \qquad \text{Eq.33}$$

3.4.8 Shear stress at the wall (flow equation)

Frictional pressure loss is proportional to shear stress at the wall (τ_w) as indicated by the fluid-modeldependent flow equation. The flow equations for Bingham-plastic and Herschel-Bulkley fluids are complex and need iterative solutions; nevertheless, they can be approximated by an expression that has the same recognizable form as the constitutive equations**.[24]** For τ_y = 0, the flow equation yields an exact solution for power-law fluids. If τ_y = YP, then n = 1 and the flow equation simplifies to the Bingham-plastic expression commonly employed in drilling.

$$\tau_f = \left(\frac{4-\alpha}{3-\alpha}\right)^n \tau_y + k\gamma_w^n \quad \text{(viscometer units)} \quad \text{Eq.34}$$

$$\tau_w = 1.066\tau_f \quad \text{(engineering units)} \quad \text{Eq.35}$$

3.4.9 Friction factor

Pressure loss in pipes and annuli is proportional to the Fanning friction factor f which is a function of generalized Reynolds number, flow regime, and fluid rheological properties.

3.4.9.1 Laminar-flow friction factor

When employing the generalized Reynolds number (N_{ReG}), the laminar-flow friction factors (flam) for pipes and concentric annuli are merged into a single relationship.

$$f_{lam} = \frac{16}{N_{ReG}} \quad \text{Eq.36}$$

3.4.9.2 Transitional-flow friction factor

An empirical equation consistent with the critical Reynolds number N_{CRe} can be used to calculate the transitional-flow friction factor f_{trans}

$$f_{trans} = \frac{16N_{ReG}}{N_{CRe}^2} \quad \text{Eq.37}$$

3.4.9.3 Turbulent-flow friction factor

The Blasius form of the turbulent-flow friction factor fturb for non-Newtonian fluids is determined by the generalized Reynolds number N_{ReG} and the rheological parameter n_P. Constants a and b are calculated using curve fits to data from power-law fluids. **[25]**

$$F_{turb} = \frac{a}{N_{Reg}^b} \quad \text{Eq.38}$$

Where,

$$a = \frac{log_{10}(n_p)+3.93}{50} \quad \text{Eq.39}$$

$$b = \frac{1.75-log_{10}(n_p)}{7} \quad \text{Eq.40}$$

CHAPTER 3:

A REVIEW OF EFFECTS OF OIL-WELL PARAMETERS IN ESTIMATING ANNULAR PRESSURE LOSSES

1 Introduction:

Hydraulic parameter design is essential for safe and efficient drilling, and capturing the flow field characteristics is the basis of the hydraulic parameters. However, the flow in annuli is complex because of many variables, such as drillstring eccentricity, rotation, drilling mud rheology, and annular cross-section size.

2 Effect of Pipe Roughness

The Fanning Equation (Eq.41) describes the pressure losses in turbulent flow of a Newtonian fluid in pipe, and the friction factor "f" determined by this equation is known as the Fanning friction factor. The operational parameters can be used to calculate all of the terms in this equation except the friction factor. The friction factor in turbulent flow depends on the Reynolds number and pipe roughness.

$$\frac{dp}{dl} = \frac{4fV^2\rho}{2D} \qquad \text{Eq.41}$$

Colebrook **[26]** established an empirical correlation (Eq. 42) for determining friction components in fully developed turbulent flow in circular pipes. The Colebrook equation is a reference standard for estimating the friction factor **[27]**. This equation, while accurate, is an implicit equation. This means that the friction factor occurs both within and outside of the log term in Colebrook's calculation. The friction factor can be solved numerically, iteratively, or using a graph to determine "f". The Moody/Fanning/Stanton graphic **[28]** depicts the friction factor against the Reynolds number on log-log paper.

$$\frac{1}{\sqrt{f}} = \left[-4\log 0.269\frac{\epsilon}{D} + \frac{1.255}{N_{Re}\sqrt{f}}\right] \qquad \text{Eq.42}$$

Where

f: is the friction factor.

$\frac{\epsilon}{D}$: is the relative roughness.

ϵ: is the equivalent sand-grain roughness.

D: is the hydraulic diameter of the pipe.

N_{Re}: is the Reynolds number.

Colebrook and White developed another generally recognized implicit equation (Eq. 43) by combining Prandtl's formula (Eq. 44) for smooth pipes with von Karman's formula for the totally rough regime (Eq.45) **[29]**. Many explicit formulae have been proposed, but some are inaccurate or not simple enough.

$$\frac{1}{\sqrt{f}} = -2\log\left[\frac{\epsilon}{3.7D} + \frac{2.51}{N_{Re}\sqrt{f}}\right] \quad \text{Eq.43}$$

$$\frac{1}{\sqrt{f}} = 2\log\left[\frac{N_{Re}\sqrt{f}}{2.51}\right] \quad \text{Eq.44}$$

$$\frac{1}{\sqrt{f}} = \log\left[\frac{3.7D}{\epsilon}\right] \quad \text{Eq.45}$$

The modified Moody **[30]** friction factor is a basic version of explicit equation seen in drilling literature. This equation allows for easy comparison of laminar, transitional, and turbulent regimes, regardless of geometry **[31].** The original Moody correlation, discovered in 1947, is valid across all Reynolds number and relative roughness levels. The Moody original friction factor connection is depicted in equation (6). Equation (7) expresses the modified friction factor, which has a roughness of 0.00001.

$$f_t = 5.5*10^{-3}\left[1 + \left(2 * 10^4 \frac{\epsilon}{D} + \frac{10^6}{N_{Rep}}\right)^{1/3}\right] \quad \text{Eq.6}$$

$$f_t = 0.001375\left[1 + \left(2 * 10^4 \frac{0.00001}{D} + \frac{10^6}{N_{Rep}}\right)^{1/3}\right] \quad \text{Eq.7}$$

Another explicit equation is the Churchill equation (Eq. 48), which was proposed by Churchill **[32]** in 1973. This equation applies solely to the turbulent regime **[33].** Chen's **[34]** correlation (Eq. 49) is likewise an explicit form of the Colebrook-White equation and provides comparable precision to the Colebrook-White equation used to generate the friction factor chart extensively used in the petroleum sector **[35]**. Haaland's **[29]** explicit equation (Eq. 50) is also employed in the drilling sector. The Haaland equation is one of the fastest and most accurate correlations among the others **[36]**. The application range follows the Colebrook equation: $0 < \frac{\epsilon}{D} < 0.05$ and $3000 < N_{Re} < 108$.

$$\frac{1}{\sqrt{f}} = -2\log\left[\frac{\epsilon}{3.71} + \left(\frac{7}{N_{Re}}\right)^{0.9}\right] \quad \text{Eq.48}$$

$$f = \left[-4log\left[\frac{\epsilon}{3.7065} - \frac{5.0452}{N_{Re}}\ log\left[\frac{\epsilon^{1.1098}}{2.8257} + \left(\frac{7.149}{N_{Re}}\right)^{0.8981}\right]\right]\right]^{-2} \quad \text{Eq.49}$$

$$\frac{1}{\sqrt{f}} = -1.8\log\left[\left(\frac{\epsilon}{3.7D}\right)^{0.9} + \frac{6.9}{N_{Re}}\right] \quad \text{Eq.50}$$

For Power-Law fluids, the Colebrook correlation does not produce correct findings, hence the Dodge and Metzner **[37]** correlation is employed instead. Equation (51) represents the Dodge and Metzner correlation. Dodge and Metzner conducted an extensive experimental and theoretical research on turbulent flow in non-Newtonian smooth pipes. They extended von Karman's research on turbulent flow friction factors to include Power-Law fluids. This correlation has been widely used in the oil and gas industry, however it tends to overestimate the frictional pressure loss **[28, 38].**

$$\sqrt{\frac{1}{f}} = \frac{4}{n_p^{0.75}}\log\left[N_{Re}f^{\left(1-\frac{n_p}{2}\right)}\right] - \frac{0.395}{n_p^{1.2}} \quad \text{Eq.51}$$

It would be extremely difficult to routinely assess pipe wall roughness when the pipe is in use **[39].** Drilling fluids are relatively viscous, with Reynolds numbers rarely exceeding 100,000. In most wellbore geometries, the relative roughness is less than 0.0004 **[28].** A straight-line approximation to the Colebrook function on a log-log plot is available for smooth pipes with Reynolds numbers ranging from 2100 to 100,000. Blasius **[40**] first published this approximation, which is represented by equation 52.

$$f = \frac{0.0791}{N_{Re}^{0.25}} \quad \text{Eq.52}$$

As a result, most academics employ empirical relationships to derive the friction factor. Moore, Adams, Rabia, Bourgoyne et al., and Carden et al. **[39,41]** study the turbulent flow of PL and Bingham Plastics (BP) similarly. However, the resulting turbulent flow equations differ significantly because the friction factor and Reynolds number were calculated using different relationships. Moore's linear relationship between the friction factor and the Reynolds number ($f = 0.046/Re^{0.2}$) differed from those employed by Adams, Bourgoyne et al. ($f = 0.0791/Re^{0.25}$), and Rabia. Carden et al. employed two different linear correlations ($f = 0.0458/Re^{0.19}$ and $f = 0.058/Re^{0.22}$). The Blasius form of the turbulent-flow friction factor for non-Newtonian fluids depends on the Reynolds number N_{Re} (Eqs. 53 and 54) and the PL rheological parameter "n_p". The formulas for "a" (Eq. 55) and "b" (Eq. 56) are

based on curve fits of data obtained from PL fluids **[31,42]**. API **[43]** incorporated these values for use in the Blasius equation for estimating turbulent flow friction factors in API RP 13D recommended practice.

$$f_t = \frac{a}{N_{Rep}^b} \qquad \text{Eq.53}$$

$$N_{ReG} = \frac{\rho V^2}{19.36\tau_w};\ N_{Rep} = \frac{928\rho D_p}{\mu_{ep}} \qquad \text{Eq.54}$$

$$a = \frac{logn_p + 3.93}{50} \qquad \text{Eq.55}$$

$$b = \frac{1.75 - logn_p}{7} \qquad \text{Eq.56}$$

The laminar flow friction factor for pipes and concentric annuli is often defined in equation (57), but the transitional flow friction factor can be approximated using the frequently accepted definition for critical number (Eq.58). Metzner and Reed **[44]** proposed Equation (57) for non-Newtonian pseudoplastic fluids in laminar flow in smooth pipes.

$$\text{Laminar flow: } f_l = \frac{16}{N_{ReG}} \qquad \text{Eq.57}$$

$$\text{Transitional flow: } f_{tr} = \frac{16N_{ReG}}{(3470-1370)^2} \qquad \text{Eq.58}$$

Where: NReG is the generalized Reynolds Number defined previously (Eq. 54).

3 Effect of Simplified Hydraulic Diameter

During annular flow, shear forces operate between the fluid and the outside of the drillpipe, as well as the interior diameter of the wellbore. For concentric annuli, the equivalent diameter can be used to express the conduit geometry. Pipe flow equations can be used to annular geometry to calculate the Fanning friction factor by substituting an equivalent diameter for the pipe diameter. Many research have been conducted to convert annular flow to pipe flow by determining an effective equivalent diameter.

Several comparable diameter definitions are offered, but two formulae are commonly employed **[45, 28]**. The first equation (Eq. 59) is based on hydraulic radius, which is the ratio of cross-sectional area to wetted perimeter in a flow channel. The equivalent diameter is four times the hydraulic radius, while for a concentric annulus, it is the difference between the internal diameters of the inner conduit ($D_{hyd} = (D_h - D_p)$). If there is no inner pipe, $D_p = 0$. The

equivalent hydraulic diameter is correctly reduces to the inner diameter of the outer pipe (Dh). API incorporated this terminology in its recommended practice RP 13D, which is referenced in key drilling textbooks **[39, 46, 63].** Bourgoyne et al. suggest that the widespread adoption of this definition is most likely owing to the method's simplicity rather than its superior accuracy. The slot flow approximation for annulus **[28]** is the second most widely used equivalent diameter equation (Eq. 60). The second equivalent diameter equation, Dhyd = 0.816(D_h-D_p), is used by the Society of Petroleum Engineers.

$$D_{hyd} = \frac{4A_{ann}}{P_{wet}} = 4\frac{\frac{\pi}{d}(D_h^2 - D_p^2)}{\pi(D_h + D_p)} = D_h - D_p \qquad \text{Eq.59}$$

$$D_{slot} = 0.816(D_h - D_p) \qquad \text{Eq.60}$$

Where:

A_{ann}: the cross sectional area of the annulus.

P_{wet}: is the wetted perimeter of the annulus.

D_h: is the inner diameter of the wellbore.

D_p: is the outer diameter of the drillpipe.

Several different hydraulic diameter estimations are documented in the literature and have been applied in practice. Lamb **[47]** presents one expression for the equivalent diameter, which is illustrated in equation (Eq. 61), by viewing the flow system as a fluid shell with radius r. Crittendon discovered another equation empirically, which is represented in equation (62) **[48]**. Langlinais et al. **[49]** investigated the impact of "hydraulic diameter", "slot approximation", and "Crittendon criteria" on Bingham Plastics (BP) and Power Law (PL) pressure losses. The Crittendon criteria, together with the BP model, provided the most accurate pressure loss prediction for all fluid samples. Jensen and Sharma **[50]** compared several friction factor and equivalent diameter definitions and discovered that for BP, the "hydraulic diameter" utilized with Chen correlation provided the best fit to experimental pressure loss data. The best estimate for PL was obtained using the "hydraulic diameter" with the Blasius correlation. Demirdal and Cunha **[51]** conducted a comparative investigation of pressure losses using the previous four diameter definitions. Annular pressure losses are calculated using the BP, PL, DPL, and YPL rheological models. For all four equivalent diameters used, BP-based pressure losses exceeded PL. Pressure losses based on narrow slot and Lamb's equivalent diameter are identical across all rheological models and flow speeds

(200 gpm to 1000 gpm). Furthermore, these two approaches result in higher pressure losses than the "hydraulic diameter" and the "Crittendon diameter". According to Dosunmu and Shah **[38]**, the "hydraulic diameter" concept of comparable diameter for an eccentric annulus is the most effective for describing friction.

$$D_{Lamp} = \sqrt{D_h^2 + D_p^2 - \frac{D_h^2 + D_p^2}{ln\left(\frac{D_h}{D_p}\right)}} \qquad \text{Eq.61}$$

$$D_{crittendon} = \frac{\sqrt[4]{D_h^4 - D_p^4 - \frac{\left(D_h^2 + D_p^2\right)^2}{ln\left(\frac{D_h}{D_p}\right)}} + \sqrt{D_h^2 + D_p^2}}{2} \qquad \text{Eq.62}$$

There are additional lesser-known equivalent diameters that have been created theoretically or empirically, such as the Petroleum Engineering approach (Eq. 63), Meter and Bird (Eq. 64), Reed and Pilehvari (Eq. 65), and Jones and Leung (Eq. 66) **[52].** The Petroleum Engineering concept was created using gas flow equations, however it provides appropriate results when applied to liquids, frequently yielding an effective diameter that is 40% higher than the "hydraulic diameter". Meter and Bird's definition applies to laminar and turbulent flow of Newtonian fluids in a concentric ring. Reed and Pilehvari's definition is based on the fluid's annular geometry and rheology. The model produces good results with YPL fluids. Jones and Leung's definition is the product of the "hydraulic diameter" plus a form factor defined by the Meter and Bird equation. Anifowoshe and Osisanya **[52]** studied the effect of both less popular and more popular definitions on pressure loss calculations. They concluded that the pressure estimation is strongly influenced by the equivalent diameter criteria utilized. The "hydraulic diameter" definition provided the most accurate estimation of pressure loss for PL fluids under laminar flow circumstances.

$$D_{Pet\ Eng} = \sqrt[5]{\left(D_h^2 + D_p^2\right)^2 * \left(D_h^2 - D_p^2\right)^2} \qquad \text{Eq.63}$$

$$D_{Meter\text{-}Bird} = D_h(1 - K)Ø;\ Ø = \frac{1}{1-K^2}\left[(1 + K^2) - \frac{1-K^2}{ln\left(\frac{1}{K}\right)}\right];\ K = \frac{D_p}{D_h} \qquad \text{Eq;64}$$

$$D_{Reed\text{-}Pilehvari} = \frac{D_h - D_p}{G};\ G = \left(\frac{1+Z}{2}\right)\frac{[n(3-Z)+1]}{[n(4-Z)]} \qquad \text{Eq.65}$$

$$Z = 1\text{-}\left[1 - \left(\frac{D_p}{D_h}\right)^{y}\right]^{1/y};\ y = 0.37n^{-0.14}$$

$$D_{jones\text{-}leun} = \text{Ø}D_e \qquad \text{Eq.66}$$

4 Effect of Tool Joint Restrictions:

The tool joint is a necessary part to extend the drill pipe. These components are manufactured separately from the pipe body and then welded to the pipe at a manufacturing plant. The tool joints offer strong, high-pressure threaded connections that can withstand drilling and repeated tightening and loosening.**[53]**

Tool joints have a smaller internal diameter (ID) than the pipe body. This restricts flow in pipes through contraction and expansion of the fluid as it enters and exits. The pressure loss caused by entry into the tool joint is small compared with the exit losses **[53].** They have larger ODs than the pipe body. As a result, the annulus clearance across a tool joint is smaller than that across the pipe body, causing some resistance to flow **[54].** On the other hand, tool joints have a larger outside diameter, which affects the annulus geometry between the drill pipe and the casing/hole, resulting in significant turbulence and fluid acceleration, which creates additional viscous dissipations and pressure losses **[53,55]**. However, the effect is minimal because fluid velocity is so low in the annulus **[54].**

Jeong and Shah **[45]** The study examined how tool joints affect annular friction pressure using water and polymeric fluids. The tool joint was shown to have a substantial effect on annular friction pressure. This impact increased friction pressure by 29% at 5 bbl/min and up to 75% at 8.5 bbl/min for fluid flow in a 5 1/2-in - 2 1/2-in annulus (Figure 3.1). Hemphill et al. **[61]** found less pressure losses, with results indicating that the tool-joint can increase annular loss by up to 12%.

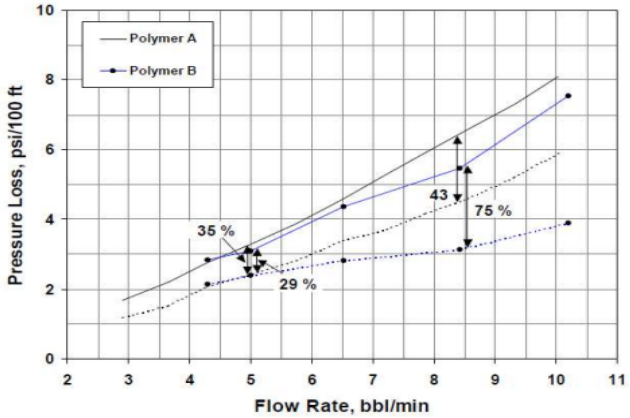

Figure 3. 1 - Effect of Tool-Joint on frictional pressure loss [45]

In another study by Shihui SUN, Tie YAN, Xiaowen YU, Guoqing YU

4.1 THEORETICAL MODEL OF ANNULUAR PRESSURE LOSS:

The total annular friction pressure loss including: ΔP_{fl} pressure loss across the tool-joint that doesnot account for the contraction and expansion losses; and ΔP_{f2} pressure loss due to tool-joint contraction and expansion, as shown in Figure 3. Hence:

$$\Delta P_f = \Delta P_{fl} + \Delta P_{f2} \quad \text{Eq.67}$$

The pressure loss $\Delta Pf1$ includes pressure losses in the narrow and wide regions of the tool joint. Therefore, $\Delta Pf1$ is calculated as the sum of these two components:

$$\Delta P_{fl} = \Delta P_N + \Delta P_W = \frac{4\,\tau_{w,N}\,L_N}{D_{hyd,N}} + \frac{4\,\tau_{w,W}\,L_W}{D_{hyd,W}} \quad \text{Eq.68}$$

Under laminar flow condition, for power law fluids, the wall shear stress in the annulus can be estimated using the narrow slot approximation method as:

$$\tau_W = K\left[\frac{12v}{D_{hyd}}\left(\frac{2n+1}{3n}\right)\right]^2 \quad \text{Eq;69}$$

For turbulent flow, wall shear stress is calculated as:

$$\tau_W = \frac{1}{2} f\rho v^2 \quad \textbf{Eq.70}$$

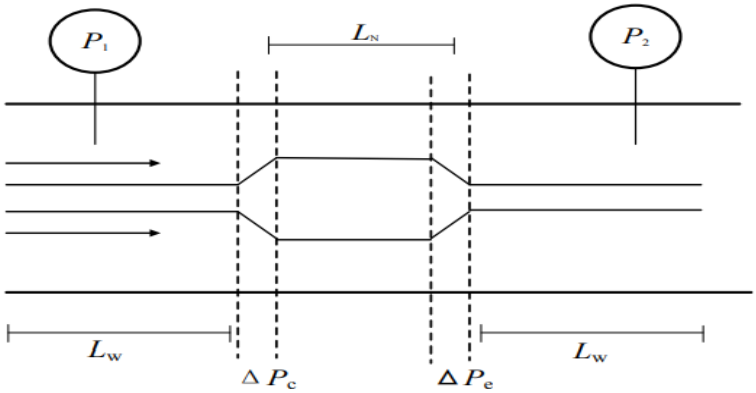

Figure 3. 2 - Schematic of tool-joint

Where f is the fanning friction factor. It can be estimated using the following correlation. For smooth pipe, friction factorcan be calculated by Dodge and Metzner equation **[13]**

$$\frac{1}{f^{0.5}} = \frac{4}{n^{0.75}} \log\left[Re\, f^{\left(1-\frac{n}{2}\right)}\right] - \frac{0.4}{n^{1.2}} \qquad \text{Eq.71}$$

For rough pipe, fanning friction factor is calculated as:

$$\frac{1}{\sqrt{f}} = -4log_{10}\left(\frac{1.255}{Re\sqrt{f}} + \frac{\varepsilon}{3.7d}\right) \qquad Eq.72$$

The hydraulic diameters of the narrow and wide parts of the tool-joint are determined as:

$$D_{hyd,N} = D_{ci} - D_{TJ}$$

$$D_{hyd,W} = D_{ci} - D_{po}$$

where,

D_{ci}: the inner diameter of casing, m;

D_{po}: the outer diameters of the drillpipeand tool-joint, respectively, m;

$$\Delta P_{f2} = \Delta P_c + \Delta P_e \qquad \text{Eq.73}$$

where,

ΔP_c: the pressure loss due to tool-joint contraction and expansion, respectively, Pa;

Contraction and expansion effects of the tool-joint are modeled using the same definition as Jeong and Shah. Accordingly, the contraction pressure loss, ΔP_c, is:

$$\Delta P_c = \rho \times K_c\left(\frac{v_N^2}{2g}\right) \qquad \text{Eq.74}$$

where, K_c is the contraction head loss coefficient. For squared tool-joint, the contraction head loss coefficient is:

$$K_c = \left(1 - \frac{A_N}{A_W}\right)^2 \qquad \text{Eq.75}$$

For tapered tool-joint, the contraction head loss coefficient is calculated as:

$$K_c = 0.5\sqrt{\sin\frac{\theta}{2}(1 - K^2)} \qquad \text{Eq.76}$$

Similarly, the expansion pressure loss ΔP_e can be defined as:

$$\Delta P_e = \rho \times K_e\left(\frac{v_W^2}{2g}\right) \qquad \text{Eq.77}$$

where, K_e is the expansion head loss coefficient, which can be determined for both squared and tapered tool-joint as:

$$K_e = \left(\frac{A_W}{A_N} - 1\right)^2 \qquad \text{Eq.78}$$

Applying the energy balance, the pressure difference between Point 1 and Point 2 (i.e. pressure loss) is expressed as:

$$\Delta P = \frac{\rho}{2g} v_N^2 \{ K_c + K_e \left(\frac{A_N}{A_W}\right)^2 \} + \Delta P_{fl} \qquad \text{Eq.79}$$

Where,

ρ: density of the fluid, kg/m3;

v_N: the fluid mean velocity in the narrow area around the tool-joint, m/s.

A_N, A_W: the areas of the narrow and wide sections of the tool joints, respectively, m^2.

Shihui SUN, Tie YAN, Xiaowen YU, Guoqing YU, Simulated well consists of a 304.8 mm long section (2.875' ×5.5' annulus) with tool-joint (60.96 mm long and 38.1 mm OD). Drilling fluid density is 1000 kg/m^3, flow pattern index is 0.6, consistency coefficient is 0.48Pa•S^n. Annulus friction pressure loss with and without tool-joint is calculated respectively using the model in **[57].** And the effect of tool-joint on annular pressure loss is analyzed.

Tool-joint Effect on the Annular Pressure Loss: Pressure loss from the sections with and without tool-joint are plotted in (Fig.3.3). Results show strong hydraulic resistance created by the tool-joint that increases the local annular pressure loss significantly as the flow rates increases. Annular pressure loss with tool-joint increased by 61% at 14 l/min and 100% at 120 l/min.

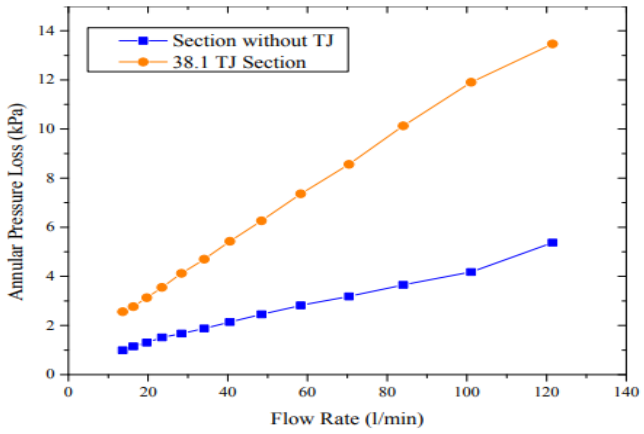

Figure 3. 3 - Comparison of annular pressure loss with and without tool-joint for different flow rates [57]

Similarly, Enfis **[58]** conducted theoretical and experimental work to investigate the hydraulic effects of both rotating and non-rotating tool-joints on annular pressure losses. Annular flow experiments were carried out for different flow rate, fluid rheology, annular geometry, rotation speed of the inner pipe. The pressure loss gradient around tool-joints increases significantly depending on fluid properties and flow geometries. The overall effect of the tool-joint on annular pressure ranged from 11% to 31%. The contraction and expansion parts of the tool-joint create strong flow disturbances and turbulent flow conditions, causing the pressure loss to increase. The fluid velocity in the narrow annulus of a tool-joint also increases. **[59, 58,60]**

5 Effect of Drillstring Rotation:

Rotary drilling requires pipe rotation since it performs a variety of purposes. Overall, the drilling community believes that pipe rotation aids in hole cleaning, particularly in horizontal and severely deviated wellbores **[56,61].** However, there have been few studies to describe the influence of pipe rotation on frictional pressure loss. Recent research has demonstrated that drillstring rotation has a considerable impact on pressure loss, especially for slim hole, long reach, horizontal, and highly deviated drilling applications. Drillpipe rotation has a significant impact on fluid characteristics, flow rates, diameter ratio, and eccentricity. Drillpipe rotation, especially at moderate rotation rates, produces unstable flow and facilitates the transition from laminar to turbulent flow **[55,60]**. According to Saasen **[60],** turbulences can occur due to pipe rotation even in the absence of axial flow, and the transversal motion of the drillstring generates vortices that destabilize the flow. As a result, the annular frictional pressure loss increases even as the drilling fluid thins due to higher shear rate. Several research have revealed a mixed effect of drill pipe rotation.

McCann et al. **[62]** conducted flow experiments in narrow annuli to collect data on the effects of pipe rotation, flow regime, fluid characteristics, and eccentricity on pressure loss in narrow annuli. The study found that increasing pipe rotation in turbulent flow increases pressure loss, while increasing pipe rotation in laminar flow decreases it. Other studies have found that increasing the rotation speed of PL fluids reduces annular pressure loss at low flow rates, but increases it at high flow rates **[63,64]**. However, Hansen and Sterri **[65]** found that for laminar flows, when the Taylor number exceeds the critical Taylor number (the Taylor number of a flow at the commencement of Taylor vortices), friction pressure loss increases with rotation speed. Otherwise, pressure loss diminishes as pipe rotation speed increases. Ozbayoglu and Sorgun **[67,68]** found that annular pressure loss increased with rotation,

particularly at low Reynolds numbers. However, when the flow rate increases, the influence of pipe rotation on annular pressure loss decreases and eventually becomes negligible.

Minghu Nie et al. **[68]** they performed three types of CFD simulations (drilling rotation, eccentricity, and annular gap) to demonstrate the flow field characteristics and the annulus pressure losses at the drillstring joint. The investigation method and results would help guide the design of drilling hydraulic parameters. Drillstring Rotation influence flow field and pressure losses at drillstring joints, Simulation results indicate that the fluid pressure loss increases significantly with the drillstring rotational rate (Figure 3.4). The reason is that the fluid disturbance inertia at the rotating joint will form significant viscous resistance, resulting in increased fluid resistance. Therefore, neglecting the drillstring rotation will inevitably form a significant deviation in the hydraulic calculation, which will bring certain risks to drilling design and construction.

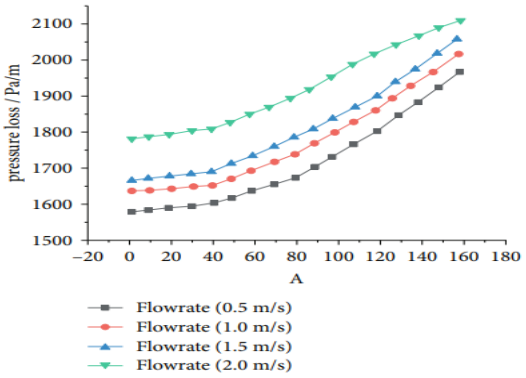

Figure 3. 4 - Effect of rotation on the pressure loss with various flowrates.[68]

Based on numerical simulations, Ooms et al. **[69]** shown that in the case of a concentric drillpipe, rotation has no effect on the axial pressure drop for a stationary, fully developed laminar flow of a Newtonian liquid. However, when the drillpipe is positioned eccentrically, the axial pressure loss increases with rotation speed. Wei et al. **[70]** reproduced these results for non-Newtonian fluids using the full-scale Tulsa University Drilling Research Project (TUDRP) flow loop. Wei et al. found that increasing inner pipe rotation resulted in a rise in annular frictional pressure loss, particularly in experiments without centralizers. This contradicted the results of their theoretical model. This impact was linked to the drillpipe's lateral motion during rotation, which causes lateral flow in the annulus and so disrupts the laminar flow. Flow tests were performed using centralizers to guarantee that the drillpipe rotated axially without moving laterally. The results suggest that increasing pipe rotation reduces annular frictional pressure loss. The primary cause of this effect is thought to be shear thinning and a fall in perceived viscosity of PL fluids. This effect was not prevalent in flow

testing without centralizers because pipe rotation causes less shear thinning than pipe lateral motion. Drillpipe rotation affects annular pressure loss depending on mud characteristics, flow rate, wellbore shape, and rotary speed.

The increase in annular pressure loss is more pronounced in thin mud with high pipe rotary speed in an eccentric pipe configuration. The TUDRP flow loop is designed to approximate real drilling situation with 41/2-in drillpipe and 8-in transparent acrylic outer pipe with a total length of 85 ft. The tested polymeric fluids have follow the PL model with "n" values range from 0.4228 to 0.7582 and "K" values range from 0.007 to 0.039 lb.sn /ft2 . Drillpipe rotary speeds range from 0 to 120 revolution per minute (rpm). Eccentricities range from 0 to 0.5 and flow rates range from 150 to 350 gallon per minute (gpm). Laminar flow is maintained in all tests.

A variety of field investigations have been conducted to assess the impact of pipe rotation on annular friction pressure losses. Separate studies conducted at drilling sites in the North Sea **[62]** investigated the effects of drillpipe rotation while circulating and rotating at various rates inside casing (without cuttings), and the results were analyzed in terms of changes in ECD calculated from downhole pressure tool data. In general, increasing rotating speed leads to an increase in pressure losses. Mobil drilled the Pando #1 Slim Hole well in Bolivia's Madre de Dios region. Hydraulic testing at this well confirmed that standpipe pressure is dependent on annular geometry, pipe rotation, and fluid characteristics **[62].** Figure 3.5 indicates that the standpipe pressure in Pando #1 grew dramatically as pipe rotations increased.

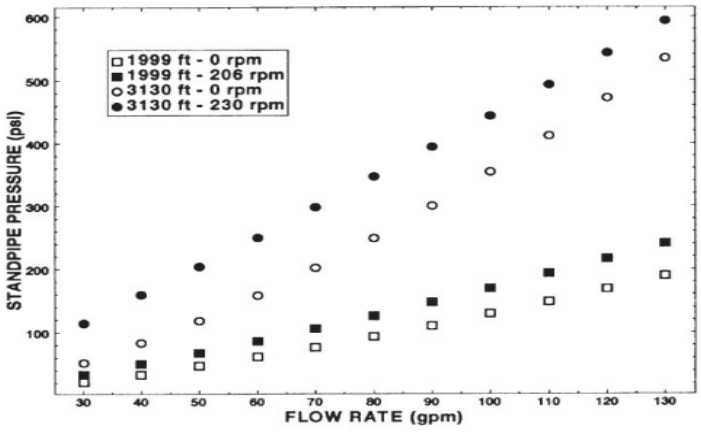

Figure 3. 5 - Effect of pipe rotation on standpipe pressure, Pando #1 slim hole well [62]

Wei et al. **[67]** examined pressure during drilling data from three extended reach wells drilled in Europe. Pipe rotation caused an increase in annular pressure loss from 66% to 147%. Furthermore, the effect of drillpipe rotation on increasing ECD is larger when axial flow is low

and decreases as axial flow increases. This effect becomes more noticeable when the gaps narrow (increasing Dp/Dh), and it can be rather dramatic in slim hole drilling operations [**54,53, 71].**

Furthermore, the influence of drillpipe rotation on annular pressure and ECD has been studied theoretically. Computer models show that the shear-thinning effect generated by pipe rotation on PL fluids reduces annular frictional pressure loss in both concentric and eccentric pipe configurations. The pressure reduction is greatest for concentric pipe configurations **[67].** However, Hemphill et al. **[72]** discovered that increasing drillpipe rotation speed at constant annular velocity resulted in a non-linear increase in ECD. Instead of eccentricity, the ratio of the drillpipe's outer diameter to the interior diameter of the hole or casing (Dp/Dh) was discovered to be a useful modelling parameter. This is due to the fact that drillpipe eccentricity cannot be determined with certainty at any given time while drilling. Calculation errors are evident when the improper level of drillpipe eccentricity is employed, as this might alter the local velocity distribution in the annulus. A potential solution to this difficulty is to base all computations on diameter ratios (Dp/Dh) **[58, 61].**

As shown from the above Annular pressure loss has been found to increase due to rotation. Here we will demonstrate a simplified method[24] to estimate rotation effect on pressure loss **[74].** The correlation is:

$$\Delta P_R = 0.00001\ N\ (\ -1.0792(\frac{D_1}{D_2}) + 17.982(\frac{D_1}{D_2})^2)\ L \qquad \text{Eq.80}$$

As seen, method simply accounts for geometry factor and rotation speed. The drawback could be that fluid rheology effect is not included as parameter.

6 Effect of Cuttings Accumulations:

cuttings are generated by the bit during drilling operation, they must be removed from the well. This task is normally achieved by circulating the so called drilling fluid down the drillstring and via bit nozzles, flushing the bit teeth, sweeps and/or entrains cuttings up the annulus to the surface.This affect the drilling fluid density and causes greater annular pressure losses than calculated. Furthermore, solid content raises the PV of BP fluids, which is factored into pressure loss formulae for BP fluids. Increased penetration rates, decreased mud carrying capacity, and poor solid control resulted in a higher concentration of these solids in the annulus, which had a bigger effect on mud density and rheology. Cuttings accumulate mostly at highly deviated wellbores. These cuttings can be found in fixed or moving beds on the wellbore's

lower side **[56].** Cuttings tend to be transported with a lower velocity than the mud, which leads to cuttings accumulation and cuttings bedding, which increases the pressure loss further**[75].**Cuttings bedding reduces hydraulic diameter and flow area, which increases friction pressure loss. As a result, in real-world drilling settings, cuttings composition, among other factors, will influence annular pressure loss.

Normally, equivalent circulation densities (ECD) are estimated using the hydrostatic pressure and frictional pressure drop in the annulus, but the cuttings concentration is not taken into account. This could lead to underestimation of ECD levels. Correct ECD is anticipated when cuttings concentrations and slide velocity of cuttings are taken into account, especially for vertical and near vertical annuli **[76]**. Figure 3.6 depicts equal circulation densities with and without cuttings.

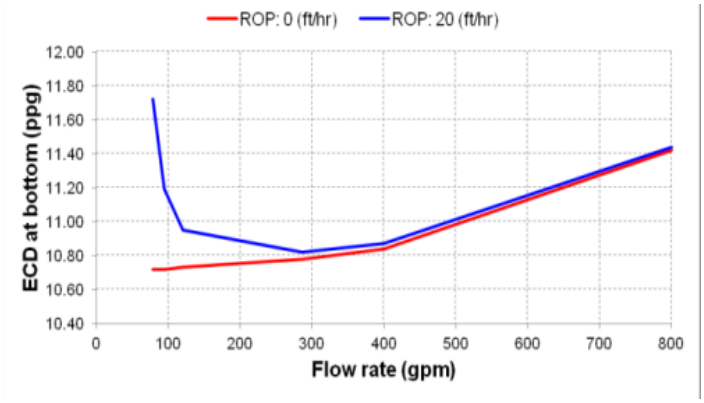

Figure 3. 6 - ECD at bottom with/without cuttings[76]

Kummen and Wold **[75]** investigated the relationship between rapid changes in cuttings concentration and the resulting changes in pressure loss, utilizing standpipe pressure as a pressure indicator. Drilling data was acquired from two North Sea wells. There was a correlation discovered between the change in rate of penetration (ROP) and the response to standpipe pressure. However, calculations show that the variation in pressure loss cannot be explained only by cutting bedding, viscosity and density changes, or the weight of suspended cuttings in the wellbore. they divided the annulus into two main sections: A vertical section, where the inclination of the borehole is below 45 from the vertical line, and an inclined section, where the borehole inclination is above 45. By doing so, simplifications can be made regarding hole cleaning and cuttings transport.

6.1 Cuttings concentration in the inclined section:

Hydraulic friction pressure loss increases with fluid density. Fluid density has an effect on the friction factor f, which is a function of the Reynolds number Re (6). The effect of suspended cuttings on pressure can be studied by determining the ratio of pressure loss with and without them. Equation 26 represents friction pressure loss (ΔP_f). Equation 81 gives the friction factor (f).

$$\Delta p_f = \frac{\Delta p_f(c)}{\Delta p_f^0} = \frac{\frac{f(c)}{2}\frac{L}{d_{hyd}}\rho(c)v^2}{\frac{f^0}{2}\frac{L}{d_{hyd}}\rho^0 v^2} = \frac{f(c)\rho(c)}{f^0\rho^0} = \frac{f(c)}{f^0}\frac{\rho_m + c(\rho_c - \rho_m)}{\rho_m} \quad \text{Eq. 82}$$

6.2 Cuttings concentration in the vertical section:

The ratio of the friction pressure with and without cuttings in the vertical section is given by equation 83.

$$\Delta p_f(c_{vert}) = \frac{\Delta p_f(c_{vert})}{\Delta p_f^0} = \frac{f(c_{vert})\rho(c_{vert})}{f^0\rho^0} = \frac{f(c_{vert})}{f^0}\frac{\rho_m + c_{vert}(\rho_c - \rho_m)}{\rho_m} \quad \text{Eq. 83}$$

C_{vert}: the cuttings concentration in the vertical section

ρ_m: the mass density of the mud

ρ_c: the mass density of the cuttings

f: The friction factor

7 Eccentricity Effect

Even vertically plan and drilled wells will have sections slightly deviated from vertical. Hence, the assumption of a concentric annulus is often not realistic, particularly, for horizontal and highly deviated wellbores. Due to its weight, drill string is always expected to lie on the lower side of wellbore in inclined holes. In these situations, annular becomes eccentric.

Eccentricity is defined with a dimensionless number e which varies from 0 to a maximum value e max (more precisely +/-e max since successive points of contact are located on opposite sides). Eccentricity e is equal to zero for a concentric annulus and is equal to one for a fully eccentric annulus. A schematic of an eccentric annulus is shown in Fig 3.7

The eccentricity is given by

$$e=\frac{2\delta}{d_0-d_i} \quad \text{Eq.84}$$

Centralizers are used to achieve a near-concentric annuli, this is the case with casing centralizers that are used to keep casings from contacting the wellbore. But even with the use of centralizers, the casing between centralizers could still deform leading to contact with the wellbore. Centralization is important for its contribution and help in casing wear studies and hole cleaning particularly on the wellbore's lower side.

With centralizers or externally upset tool joints

$$e=\frac{do-d_c}{d_o-d_i} \quad \text{Eq.85}$$

where:

e= eccentricity, dimensionless

δ= distance between centers of inner and outer pipes, L

d_0 = outer pipe diameter, L

d_i = inner pipe diameter, L

d_c= centralizer or external upset diameter, L

A skewness parameter s is defined as the ratio of average annular diameter $davg$ to ΔL

$$s=\frac{davg}{\Delta L}$$

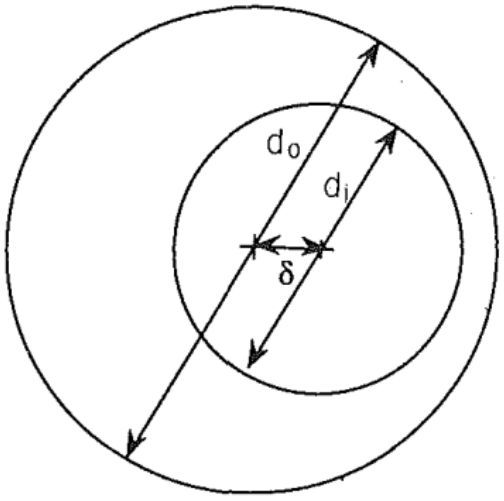

Figure 3. 7 - Eccentric annulus

The annular frictional pressure losses of vertical or near vertical well sections differ from the highly inclined and horizontal wellbores. This is because of natural tendency of the drill string to lay down on the low side of the wellbore due to gravity. Moreover, the drill string is elastic and has the possibility to wobble in the hole during rotation. It can be positioned differently in the wellbore cross section at different depths, depending on inclination and hook load **[17].** The pressure losses depend on the annulus eccentricity. Moving the drill string to the wall of the wellbore creates a bigger flow channel in the annulus, changing the direction and acceleration of the annular flow and reduces the frictional pressure losses significantly.

Many experimental studies on hydraulics of eccentric annuli have been conducted. Their results show that pressure loss decreases as eccentricity increases. Pressure losses ranging from 18 to 40% lower than those of the concentric annulus were recorded (ref photo li ta7t). A commonly used method to determine the magnitude of this reduction **[77]**is based on product of concentric annulus pressure loss and empirically derived ratio R depending on flow regimes. R is the ratio of AFP in concentric annulus to AFP in eccentric annulus. Equations to calculate R are given as

$$R_{lam} = 1 - 0.072\frac{e}{n}\left(\frac{D_1}{D_2}\right)^{0.8454} - \frac{3}{2}e^2\sqrt{n}\left(\frac{D_1}{D_2}\right)^{0.1852} + 0.96e^3\sqrt{n}\left(\frac{D_1}{D_2}\right)^{0.2527} \quad \text{Eq.86}$$

$$R_{turb} = 1 - 0.048\frac{e}{n}\left(\frac{D_1}{D_2}\right)^{0.8454} - \frac{3}{2}e^2\sqrt{n}\left(\frac{D_1}{D_2}\right)^{0.1852} + 0.285e^3\sqrt{n}\left(\frac{D_1}{D_2}\right)^{0.2527} \quad \text{Eq.87.}$$

Drill pipe eccentricity is affected by hole inclination angle, weight on bit and the size of the hole as shown in Equ 88

Well geometry and string stiffness have an important role in annular eccentricity. In deviated wells, the DP should be fully eccentric over much of the deviated wellbore. In medium inclined sections of the deviated well, such as between 0˚ - 30˚, the drill strings tend to lie on the high side of the wellbore. Meanwhile in high inclined sections or in horizontal wellbores, the DS lies on the lower side of the wellbore. Eccentricity will affect both the flow and the velocity distribution of fluids in the wellbore. It has been shown by research that the frictional pressure drop in an eccentric annulus is known to be less than the frictional pressure drops in a concentric annulus although this varies with fluid rheology type, the difference being much profound in Newtonian fluids than in non-Newtonian fluids **[78]**. Standoff is usually used to represent eccentricity expressed in percentage. An eccentricity of 100% implies a standoff of 0% and means that the inner pipe is in contact with the outer pipe or hole at the low side. Meanwhile, an eccentricity

of 0% implies a standoff of 100% and means that the inner pipe is perfectly centered in the outer pipe or wall; this is a concentric situation.

A correlation was developed by Salem and El-Din (2006) to determine the distance δ called Y_{max}

$$e = \frac{Y_{max}}{d_0 - d_i}$$

$$\delta = Y_{max}$$

$$Y_{max} = \left(\frac{5.68EI}{W.cos\Theta}\right)\left\{\left(\frac{0.176Wsin\theta(5.68EI)^{0.5}}{EI(W)cos\Theta}\sinh\frac{(X(0.176Wcos\Theta)^{0,5}}{2(EI)^{0,5}}\right.\right.$$

$$\left.\left. - \frac{(0.176Wcos\Theta)^{0,5}}{2(EI)^{0,5}}\right) + \frac{0.5X^2qsin\theta}{4EI}\right\} \quad \text{Eq.88}$$

Where

W = weight on bit, (Ib)

E = modulus of elasticity, (psi)

θ = hole inclination angle, (degree)

I = moment of inertia of the drill pipe (inch), X = drill pipe horizontal projection, 1000 inches

q = axial component of weight of drill pipe per unit length, lb/ft.

The pressure drop in eccentric annular flow is given as:

$$\left[\frac{dP_f}{dL}\right]_e = C_e\left[\frac{dP_f}{dL}\right]_C \quad \text{Eq.89}$$

$$C_e = f(e, r_i / r_0, k, \tau 0)$$

Where C_e *represents the correction factor for eccentricity*

n= flow behavior index

$\tau 0$ = Yield stress in lb/ft

K = Consistency index

8 Conclusion

In conclusion, we have discussed the importance of inderstanding these parameters and their impact on the overall drilling procces. Through the analysis of various studies and research, we have identified several key parameters that play a significant role in estimating annular pressure losses.

Based on the finding presented in this chapter, it is recommended that future researchers choose one specific parameter and conduct in-depth research on its influence on annular pressure losses starting from the base we provided

General Conclusion

This research delves into the intricate dynamics of fluid rheology and multiphase flow within non-Newtonian wellbore systems, uncovering critical insights that are essential for optimizing drilling and production operations. The study underscores the profound impact that rotation speed, flow behavior index, diameter ratio and specially the eccentricity have on wellbore performance and highlights the need for advanced approaches and technologies to manage these complexities effectively.

In this research, we focused on studying the parameters affecting annular pressure loss in non-Newtonian wellbore systems. The investigation provided significant insights into the various factors influencing pressure dynamics and flow behavior within the annular space,

In conclusion, the study highlights the significant influence of fluid rheology and multiphase flow on the pressure and flow dynamics within non-Newtonian wellbore systems, showing a synergetic effect of all studied factors on the wellbore performance. A thorough understanding and precise modeling of these factors are essential for ensuring the efficiency and safety of drilling and production operations. Continued research and technological advancements are crucial for overcoming the challenges posed by these complex systems, ultimately leading to more effective and reliable wellbore management strategies

References

[1] Reynolds, O (1886). On the Theory of Lubrication and Its Application to Mr. Beauchamp Tower's Experiments, Including an Experimental Determination of the Viscosity of Olive Oil. Philos.Trans.R.Soc. London, 177(1886): 157-234.

[2] https://www.researchgate.net/publication/330500522; 15/05/2024 21:20

[3] Krieger, I.M.; and Dougherty, I.J. (1959). A mechanism for Non-Newtonian Flow in Suspension of Rigid Spheres. Journal of Rheology 3; 137-152.

[4] Barnes, H.A. (1997). Thixotropic A Review. Journal of Non-Newtonian Fluid Mechanics, 70(1-2) :1-33.

[5] Mewis, J and Wagner, N.J (2009). Thixotropy. Advances in Colloid and Interface Science. 147-148:214-227.

[6] Pritchard, D, Wilson, S.K and McArdle, C.R (2016). Flow of a Thixotropic Fluid in a slowly Varying Channel: The Weakly Advective Regime. Journal of Non-newtonian Fluid Mechanics. 238:140-157.

[7] Livescu, S (2012). Mathematical Modelling of Thixotropic Drilling Mud and Crude Oil Flow in Wells and Pipelines.: A Review. J. Pet.Sci.Eng. 98-99(2012): 174-184.

[8] Skalle, P, (2010). Drilling Fluid Engineering. Ventus Publishing, APS, Trondheim, Norway. Pp 16-30

[9] Anawe P.A.L and Folayan, J.A (2018**).** Investigation of the Effect of Yttrium Oxide (Y_2O_3) Nanoparticles on the Rheological Properties of Water Based Mud Under High Temperature- High Pressure Environment. International Journal of Mechanical Engineering and Technology. 9(7): 545-559

[10] Ahmed S.M (2016). Effect of Temperature on the Rheological Properties with Shear Stress Limit of Iron Oxide Nanoparticle Modified Bentonite Drilling Muds. Egyptian Journal of Petroleum. 26(3) :791-802.

[11] Darley, H.C and Gray, G. R (1988). Composition and Properties of Drilling and Completion Fluids. Fifth Edition. Gulf publishing company, Houston Texas. pp 1-37.

[12] Aftab, A., Ismail, A. R and Ibupoto, Z.H (2017). Enhancing the Rheological Properties and Shale Inhibition Behavior of Water-Based Mud using Nano-Silica, Multi-Walled Carbon Nanotube and Graphene Nano-platelet. Egyptian Journal of Petroleum. Vol 26, Issue1, pp291-299

[13] Steffe, J.F. (1996). Rheological Methods in Food Process Engineering. Sixth Edition. Freeman press. East Lansing USA.ISBN 0-9632036-1-4.

[14] Folayan, J.A, Anawe, P.A.L, Abioye, P.O and Elehinafe, F.B (2017). Selecting the most Appropriate Model for Rheological Characterization of Synthetic Based Drilling Mud.International Journal of Applied Engineering Research. 12(8):7614-7629.

[15] Fann Instrument Company (2013). Model 35 Viscometer Instruction Manual, Fann Instrument Company, Houston, Texas, pp. 44.

[16] Herschel, W.H.; and Buckley, R. (1926). Konsistenzmessungen von Gummi Benzollosungen. Kolloid 39; 291-300

[17] Kummen, H.T. and Wold, A.A., 2015. The Effect of Cuttings on Annular Pressure Loss. M.Sc. thesis, NTN-Trondheim, Norwegian University of Science and Technology.

[18] ZAMORA M. Virtual rheology and hydraulics improve use of oil and synthetic-based drilling fluids. Oil & Gas J, March 3, 1997, pp. 43-55.

[19] BARANTHOL, C., ALFENOR, J. COTTERILL, M.D. and POUX-GUILLAUME, G. Determination of hydrostatic pressure and dynamic ECD by computer models and field measurements on the directional HPHT well 22130C-13, SPE 29430. SPE/IADC 1995 Drilling Conference, Amsterdam, Netherlands.

[20] FONTENOT J.E. and CLARK R.K. An improved method for calculating swab/surge and circulation pressures in a drilling well. SPE J, Oct. 1974, pp 451-461.

[21] BOURGOYNE A.T., et al. Applied drilling engineering. SPE, Richardson, Texas, 1991.

[22] ZAMORA, M. and LORD, D.L. Practical analysis of drilling mud flow in pipes and annuli, SPE 4976. SPE 1974 Annual Technical Conference, Houston, Texas,

[23] SAVINS J.G. Generalized Newtonian (pseudoplastic) flow in stationary pipes and annuli. Petroleum Transactions of AIME, 218, pp. 332.

[24] ZAMORA M. and POWER D. Making a case for AADE hydraulics and the unified rheological model, AADE-02-DFWM-HO-13. AADE 2002 Technology Conf., Apr. 2-3, 2002

[25] SCHUH F.J. Computer makes surge-pressure calculations useful. Oil & Gas J, Aug. 3, 1965, pp. 96-104.

[26] Colebrook, C.F., 1938. Turbulent Flow in Pipes, with Particular Reference to the Transition Region between the Smooth and Rough Pipe Laws. J.Inst. Civil Engs., London., JICE 11:133–139.

[27] Offor, U.H. and Alabi, S.B., 2016. Artificial Neural Network Model for Friction Factor Prediction. Journal of Materials Science and Chemical Engineering, 4, 77- 83. DOI: 10.4236/msce.2016.47011.

[28] Bourgoyne, Jr A.T., Millheim, K.K., Chenevert, M.E., Young, Jr F.S., 1986. Applied drilling engineering, SPE Textbook Series Vol. 1, ISBN: 978–1–55563–001–0, chapter 4.

[29] Haaland, S.E. 1983. Simple explicit equation for friction factor. J Hydraul Div Am Soc Civ Eng. 102, 674-677.

[30] Moody, L.F., 1947. An Approximate Formula for Pipe Friction Factors. Trans ASME 69, 1005-1006.

[31] Zamora, M., Roy, S., and Slater, K., 2005. Comparing a basic set of drilling fluid pressure loss relationships to flow-loop and field data. AADE National Technical Conference and Exhibition.

[32] Churchill, S.W., 1973. Empirical Expressions for the Shear Stress in Turbulent Flow in Commercial Pipe. AIChE J, 19, 375-376.

[33] Asker, M., Turgut, O.E., and Coban, M.T., 2014. A Review of Non Iterative Friction Factor Correlations for the Calculation of Pressure Drop in Pipes. Bitlis Eren Univ Journal of Science and Technology, 4(1), 1-8, June 2014.

[34] Chen, N.H., 1979. An Explicit Equation for Friction Factor in Pipe. Ind. Eng. Chem Fund, 18, 96-297.

[35] Guo, B. and Li, G., 2011. Applied Drilling Circulation Systems – Hydraulics, Calculations and Methods. Gulf Professional Publising – an imprint of Elsevier.

[36] Muzzo, L.E., Matoba, G.K. and Ribeiro, L.F., 2021. Uncertainty of Pipe Flow Friction Factor Equations. Mecaics Research Communication, 116, 103764. DOI: 10.1016/j.mechrescom.2021.103764.

[37] Dodge, D.G. and Metzner, A.B., 1959. Turbulent Flow of Non-Newtonian Systems." AIChE J., 5 No2, 189 – 204. DOI: 10.1002/aic.690050214.

[38] Dosunmu, I.D. and Shah, S.N., 2013. Evaluation of Friction Factor Correlations and Equivalent Diameter Definitions for Pipe and Annular Flow of Non-Newtonian Fluids. Journal of Petroleum Science and Engineering, 109, 80-86. DOI: 10.1016/j.petrol.2013.02.007.

[39] Rabia, H., 1985. Oilwell drilling engineering. Published by Graham and Trotman, Principles and Practices, chapter 5.

[40] Blasius, H. 1913. Das Aehnlichkeitsgesetz bei Reibungsvorgangen in Flussigkeiten. VDL Forsch, 131–137.

[41] Carden, R.S., Grace, R.D., and Shursen, J.L., 2004. Drilling Practice. Chapter 6, Petroskills, LLC, an OGCI Company, Tulsa, Oklahoma.

[42] Schuh, F.J. 1964. Computer Makes Surge-Pressure Calculations Useful. Oil and Gas J (3 Aug 1964) 96-104.

[43] API, American Petroleum Institute (1995). "Recommended Practice on the Rheology and Hydraulics of Oil-Well Drilling Fluids." 4th edition, (June 1995).

[44] Metzner, A.B. and Reed, J.C., 1955. Flow of non-Newtonian Fluids-Correlation of the Laminar, Transition and Turbulent Flow Regions. AIChE J. (1955) 1, No. 4, pp. 434-40.

[45] Jeong, Y. and Shah, S., 2004. Analysis of Tool Joint Effects for Accurate Friction Pressure Loss Calculations. Paper SPE 87182, presented at the IADC/SPE Drilling Conference, Dallas, Texas, 2-4 March. DOI: 10.2118/87182-MS.

[46] Moore P.L. (1986). "Drilling Practices Manal." 2nd Edition, PennWell Publishing Company, chapter 7, pp.247 - 267.

[47] Lamb, H., 1945. Hydrodyamics. 6th Edition, Dover Publications, New York City.

[48] Crittendon, B.C., 1959. The Mechanics of Design and Interpretation of Hydraulic Fracture Treatments. Paper SPE 1106-G presented at the 33rd Annual Fall Meeting of the Society of Petroleum Engineers at Houston, Texas, October 5-8, 1958. Also in J. of Petroleum Technology, pp. 21-29, October, 1959. DOI: 10.2118/1106-G.

[49] Langlinais, J.P., Bourgoyne, A.T., and Holden, W.R., 1985. Frictional Pressure Losses for Annular Flow of Drilling Mud and Mud–Gas Mixtures. Trans. AIME, 107,142–151.

[50] Jensen, T.B., and Sharma, M.P., 1987. Study of Friction Factor and Equivalent Diameter Correlations for Annular Flow of Non-Newtonian Drilling Fluids. Trans.AIME, 109, 200–205.

[51] Demirdal, B. and Cunha, J.C., 2007. Investigaton of Effect of Equivalent Diameter Definitions on Determination of Pressure Losses of Non-Newtonian Fluids in Annuli. Paper presented at the Petroleum Society's 8th Canadian International Petroleum Conference (58th Annual Technical Meeting), Calgary, Alberta, Canada, June 12-14.

[52] Anifowoshe, O. and Osisanya, S.O., 2012. The Effect of Equivalent Diameter Definitions on Frictional Pressure Loss Estimation in an Annulus with Pipe Rotation.

Paper SPE 151176 presented at the SPE Deepwater and Completions Conference and Exhibition held in Galveston, Texas, 20-21 June. DOI: 10.2118/151176-MS.

[53] Ochoa, M.V., 2006. Analysis of Drilling Fluids Rheology and Tool Joint Effect to Reduce Errors in Hydraulics Calculations. PhD dissertation, Texas A&M U., College Station, Texas.

[54] Improving drilling hydraulics estimationsa case study

[55] Ashena, R., Hekmatinia, A., Ghalambor, A., Aadnoy, B., Enget, C. and Rasouli, V., 2021. Improving Drilling Hydraulics Estimations - A Case Study. Journal of Petroleum Exploration and Production Technology (2021)11:2763-2776. DOI: 10.1007/s13202-021-01203-4.

[56] Muherei, M.A., 2003. Cuttings Transport in Horizontal and Highly Deviated Wellbores. M.Sc thesis, University Teknologi Malaysia (UTM), Johor, Malaysia.

[57] Consideration of Tool-joint Effects for Annular Pressure Loss Calculation

[58] Enfis, M.S., 2011. The Effects of Tool-Joint on Annular Pressure Loss. Msc thesis, Mewbourne School of Petroleum and Geological Engineering, Norman, Oklahoma.

[59] White W.W., Zamora M., and Svoboda, C.F., 1996. Downhole measurements of synthetic based drilling fluid in offshore well quantify dynamic pressure and temperature distributions. SPE 35057-MS, Presented at IADC/SPE Drilling Conference, 12–15 March, New Orleans, Louisiana. Vol. 12 (3), p. 149. DOI: 10.2118/35057-MS.

[60] Saasen, A., 2014. Annular Frictional Pressure Losses During Drilling – Predicting the Effect of Drillstring Rotation. Journal of Energy Resources Technology, Vol. 136, pp. 1-5.

[61] Hemphill, T. and Ravi, K., 2006. Pipe Rotation and Hole Cleaning in an Eccentric Annulus. - IADC-SPE-99150, paper presented at the IADC/SPE Drilling Conference held in Miami, Florida, USA, 21-23 February 2006. DOI: 10.2118/99150.

[62] McCann, R.C., Quigley, M.S., Zamora, M., and Slater, K.S., 1995. Effects of High Speed Rotation on Pressure Losses in Narrow annuli. J. SPE Drilling and Completion 10 (2): 96-103. SPE-26343-PA. DOI: 10.2118/26343-PA.

[63] Hansen, S.A., Rommetveit, R., Sterri, N., Aas, B., and Merlo, A., 1999. A New Hydraulic Model for Slim Hole Drilling Applications. Paper SPE 57579, presented at the SPE/IADC Middle East Drilling Technology Conference, Abu Dhabi, United Arab Emirates, 8-10 November. DOI: 10.2118/57579-MS.

[64] Roy, S. and Zamora, M., 2006. Annular Flow-Loop Studies of Non-Newtonian Reservoir Drilling Fluids. Paper AADE-06-DF-HO-03, presented at the AADE Fluids Conference, Houston, Texas, 11-12 April.

[65] Hansen, S.A. and Sterri, N., 1995. Drill Pipe Rotation Effects on Frictional Pressure Losses in Slim Annuli. Paper SPE 30488, presented at the SPE Annual Technical Conference and Exhibition, Dallas Texas, 22-25 October. DOI: 10.2118/30488-MS.

[66] Ozbayoglu, M. and Sorgun, M., 2009. Frictional Pressure Loss Estimation of Non Newtonian Fluids in Realistic Annulus with Pipe Rotation. Paper SPE 2009-042, presented at the Canadian International Petroleum Conference, Calgary, Alberta, 16-18 June. DOI: 10.2118/2009-042.

[67] Ozbayoglu, M. and Sorgun, M., 2010. Frictional Pressure Loss Estimation of Water Based Drilling Fluids at Horizontal and Inclined Drilling with Pipe Rotation and Presence of Cuttings. Paper SPE 127300, presented at SPE Oil and Gas India Conference and Exhibition held in Mumbai, India, 20-22 January 2010. DOI: 10.2118/127300.

[68] Minghu Nie, Yuchen Ye,Zheng Wang, Dandan Yuan, Xingyi Wang, and Kai Wei Flow Field and Pressure Loss Characteristics at Rotary Drillstring Joints

[69] Ooms, G.,M Burgerscentram, J.M., Kampman-Reinhartz, B.G., 1996. Influence of Drillpipe Rotation and Eccentricity on Pressure Drop over Borehole during Drilling. Eur. J. Mech. 5(1996) 695.

[70] Wei, X., Miska, S.Z., Takach, N.E., Bern, P. and Kenny, P., 1998. The Effect of Drillpipe Rotation on Annular Frictional Pressure Loss. Journal of Energy Resources Technology, Vol. 120. P. 61.

[71] Charlez, P., Easton, M., and Morrice, G., 1998. Validation of Advanced Hydraulic Modeling Using PWD Data. Paper OTC 8804, presented at the Offshore Technology Conference, Houston, Texas, 4-7 May. DOI: 10.4043/8804-MS.

[72] Ward, C. and Andreassen, E., 1998. Pressure-While-Drilling Data Improve Reservoir Drilling Performance. J. SPE Drill and Completion 13 (1): 19-24. SPE- 37588-PA. DOI: 10.2118/37588-PA.

[73] Hemphill, T. and Ravi, K., 2006. Pipe Rotation and Hole Cleaning in an Eccentric Annulus. - IADC-SPE-99150, paper presented at the IADC/SPE Drilling Conference held in Miami, Florida, USA, 21-23 February 2006. DOI: 10.2118/99150.

[74] Elmaddin Rahimov ,éàThrough Tubing Rotary Managed Pressure Drilling

[75] Kummen, H.T. and Wold, A.A., 2015. The Effect of Cuttings on Annular PressureLoss. M.Sc. thesis, NTN-Trondheim, Norwegian University of Science and Technology.

[76] Xiang, Y. and Liu, G., 2012. Impact of Cuttings Concentration on ECD during Drilling. Paper presented at the 2012 AADE Fluids Technical Conference and Exhibition held at the Hilton Houston North Hotel, Houston, Texas, April 10-11, 2012.

[77] Mario Zamora, Sanjit Roy, and Ken Slater, M-I SWACO, Comparing a Basic Set of Drilling Fluid Pressure-Loss Relationships to Flow-Loop and Field Data, paper AADE-05-NTCE-27, AADE, Houston, Texas, 5-7 April, 2005.

[78] Akrong, J.A. (2010) Effect of Pipe Eccentricity on Hole Cleaning and Wellbore Hydraulics. Master's Thesis, African University of Science and Technology, Abuja